Check for updates

A Coevolved EDS1-SAG101-NRG1 Module Mediates Cell Death Signaling by TIR-Domain Immune Receptors[OPEN]

Dmitry Lapin,[a,1] Viera Kovacova,[b,c,1] Xinhua Sun,[a,1] Joram A. Dongus,[a] Deepak Bhandari,[a,2] Patrick von Born,[a] Jaqueline Bautor,[a] Nina Guarneri,[a,3] Jakub Rzemieniewski,[a] Johannes Stuttmann,[d] Andreas Beyer,[b] and Jane E. Parker[a,e,4]

[a] Department of Plant-Microbe Interactions, Max-Planck Institute for Plant Breeding Research, 50829 Cologne, Germany
[b] Cellular Networks and Systems Biology, CECAD, University of Cologne, Cologne 50931, Germany
[c] Faculty of Statistical Physics of Biological Systems, Predictive Models of Evolution, Institute for Biological Physics, University of Cologne, Cologne 50937, Germany
[d] Department of Genetics, Institute for Biology, Martin Luther University Halle-Wittenberg, Halle 06120, Germany
[e] Cologne-Düsseldorf Cluster of Excellence in Plant Sciences (CEPLAS) D-40225 Düsseldorf, Germany

ORCID IDs: 0000-0001-9591-3950 (D.L.); 0000-0003-4581-4254 (V.K.); 0000-0001-8687-2528 (X.S.); 0000-0002-8553-6802 (J.A.D.); 0000-0002-7666-6410 (D.B.); 0000-0001-8146-8585 (P.v.B.); 0000-0002-8074-6907 (J.B.); 0000-0002-0399-9230 (N.G.); 0000-0001-7274-383X (J.R.); 0000-0002-6207-094X (J.S.); 0000-0002-3891-2123 (A.B.); 0000-0002-4700-6480 (J.E.P.)

Plant nucleotide binding/leucine-rich repeat (NLR) immune receptors are activated by pathogen effectors to trigger host defenses and cell death. Toll-interleukin 1 receptor domain NLRs (TNLs) converge on the ENHANCED DISEASE SUSCEPTIBILITY1 (EDS1) family of lipase-like proteins for all resistance outputs. In Arabidopsis (*Arabidopsis thaliana*) TNL-mediated immunity, *At*EDS1 heterodimers with PHYTOALEXIN DEFICIENT4 (*At*PAD4) transcriptionally induced basal defenses. *At*EDS1 uses the same surface to interact with PAD4-related SENESCENCE-ASSOCIATED GENE101 (*At*SAG101), but the role of *At*EDS1-*At*SAG101 heterodimers remains unclear. We show that *At*EDS1-*At*SAG101 functions together with N REQUIRED GENE1 (*At*NRG1) coiled-coil domain helper NLRs as a coevolved TNL cell death-signaling module. *At*EDS1-*At*SAG101-*At*NRG1 cell death activity is transferable to the Solanaceous species *Nicotiana benthamiana* and cannot be substituted by *At*EDS1-*At*PAD4 with *At*NRG1 or *At*EDS1-*At*SAG101 with endogenous *Nb*NRG1. Analysis of EDS1-family evolutionary rate variation and heterodimer structure-guided phenotyping of *At*EDS1 variants and *At*PAD4-*At*SAG101 chimeras identify closely aligned -helical coil surfaces in the *At*EDS1-*At*SAG101 partner C-terminal domains that are necessary for reconstituted TNL cell death signaling. Our data suggest that TNL-triggered cell death and pathogen growth restriction are determined by distinctive features of EDS1-SAG101 and EDS1-PAD4 complexes and that these signaling machineries coevolved with other components within plant species or clades to regulate downstream pathways in TNL immunity.

INTRODUCTION

In plants, immunity to host-adapted pathogens is mediated by large, diversified families of intracellular nucleotide binding/leucine-rich repeat (NLR) receptors whose members recognize specific pathogen virulence factors (effectors) that are delivered into host cells to promote infection (Baggs et al., 2017). NLRs are ATP/ADP-binding molecular switches, and their activation by effectors involves intra- and intermolecular conformational changes that lead to rapid host-gene expression changes, induction of antimicrobial pathways, and often localized cell death

called a hypersensitive response (Cui et al., 2015; Jones et al., 2016). A signature of plant NLR immunity is the induction of multiple transcriptional sectors that can buffer the host against pathogen interference (Tsuda et al., 2013; Cui et al., 2018; Mine et al., 2018; Bhandari et al., 2019). How NLR receptors initiate downstream resistance pathways in effector-triggered immunity (ETI) remains unclear.

Two major pathogen-sensing NLR receptor classes, TIR-NLRs (TNLs) and CC-NLRs (CNLs), are broadly defined by their N-terminal Toll/interleukin-1 receptor (TIR) or coil-coiled (CC) domains. Evidence suggests that these domains serve in receptor activation and signaling (Cui et al., 2015; Zhang et al., 2017). Different NLR protein families characterized in Arabidopsis (*Arabidopsis thaliana*) and Solanaceae species function together with pathogen-detecting (sensor) NLRs in ETI and thus are considered "helper" NLRs (Wu et al., 2018) that might bridge sensor NLRs and other immunity factors. Members of the *NRC* (*NLR required for HR-associated cell death*) gene family, which expanded in Asterids, signal in ETI conferred by partially overlapping sets of phylogenetically related sensor CNLs (Wu et al., 2017). Two sequence-related NLR groups, N REQUIRED GENE1 (NRG1; Peart et al., 2005; Qi et al., 2018)

and ACCELERATED DISEASE RESISTANCE1 (ADR1; Bonardi et al., 2011) signaling NLRs, were originally classified by a distinct CC domain sequence (referred to as CC_R) shared with the Arabidopsis RESISTANCE TO POWDERY MILDEW8 (RPW8) family of immunity proteins (Collier et al., 2011). This domain shows similarity to mixed-lineage kinase domain-like pseudo-kinase, a component of necroptotic cell death in mammals (Petrie et al., 2018; Jubic et al., 2019). Subsequent analysis revealed that although monocot ADR1s lack the CC_R (Zhong and Cheng, 2016), these NLRs share a phylogenetically distinct nucleotide binding domain (Shao et al., 2016; Zhong and Cheng, 2016). Studies of *nrg1* and *adr1* mutants in Arabidopsis and wild tobacco (*Nicotiana benthamiana*) revealed important roles of the genes in ETI (Peart et al., 2005; Bonardi et al., 2011; Dong et al., 2016; Qi et al., 2018; Castel et al., 2019; Wu et al., 2019). Notably, *NRG1* genes are necessary for eliciting host cell death in several TNL but not CNL receptor responses (Qi et al., 2018; Castel et al., 2019). By contrast, three Arabidopsis ADR1 proteins (*At*ADR1, *At*ADR1-L1, and *At*ADR1-L2) act redundantly in signaling downstream of CNL and TNL receptors (Bonardi et al., 2011; Dong et al., 2016; Wu et al., 2019). In resistance to bacteria triggered by the Arabidopsis sensor CNL RESISTANT TO PSEUDOMONAS SYRINGAE2 (RPS2), ADR1-family stimulated accumulation of the disease resistance hormone salicylic acid (SA) and cell death (Bonardi et al., 2011). Analysis of flowering plant (angiosperm) genomes indicated the presence of *NRG1* and *TNL* genes in eudicot lineages and loss of these genes from monocots and several eudicots (Collier et al., 2011; Shao et al., 2016; Zhang et al., 2016). By contrast, Arabidopsis *ADR1* orthologs are present in eudicot and monocot species (Collier et al., 2011; Shao et al., 2016). To date, there is no evidence of molecular interactions between sensor and helper NLRs.

All studied TNL receptors, activated by pathogen effectors in ETI or as autoactive molecules (producing autoimmunity), signal via the non-NLR protein Enhanced Disease Susceptibility1 (EDS1) for transcriptional defense reprograming and cell death (Wiermer et al., 2005; Wirthmueller et al., 2007; García et al., 2010; Xu et al., 2015; Adlung et al., 2016; Ariga et al., 2017; Qi et al., 2018). EDS1 is therefore a key link between TNL activation and resistance pathway induction. Consistent with an early regulatory role in TNL signaling, *At*EDS1 interacts with a number of nuclear TNLs (Bhattacharjee et al., 2011; Heidrich et al., 2011; Kim et al., 2012). In addition, interaction between *Nb*EDS1a and *Nb*NRG1 was recently reported (Qi et al., 2018). Together with PHYTOALEXIN DEFICIENT4 (PAD4) and SENESCENCE ASSOCIATED GENE101 (SAG101), EDS1 constitutes a small family found in angiosperms but not nonseed species, postdating the origin of *NLR* genes in plants (Wagner et al., 2013; Gao et al., 2018). Phylogenetic sampling of 16 angiosperm species indicated that *EDS1* and *PAD4* are present in eudicots and monocots, whereas *SAG101* (like *NRG1* and *TNL*s) was not detected in monocot genomes (Collier et al., 2011; Wagner et al., 2013).

The three EDS1-family proteins possess an N-terminal α/β-hydrolase fold domain with similarity to eukaryotic class-3 lipases and a unique C-terminal α-helical bundle, referred to as the EDS1-PAD4 defined (EP) domain (Protein Families [pfam] identifier: PF18117; Wagner et al., 2013).

*At*EDS1 forms exclusive heterodimers with *At*PAD4 and *At*SAG101 through N- and C-terminal contacts between the partner domains (Feys et al., 2001, 2005; Rietz et al., 2011; Wagner et al., 2013). Genetic, molecular, and protein structural evidence from Arabidopsis revealed a function of *At*EDS1 heterodimers with *At*PAD4 in basal immunity that is boosted by TNLs in ETI via an unknown mechanism (Feys et al., 2005; Rietz et al., 2011; Bhandari et al., 2019). EDS1-PAD4 basal immunity limits the growth of infectious (virulent) pathogens without host cell death and is thought to reflect a core EDS1-PAD4 immunity function (Zhou et al., 1998; Rietz et al., 2011; Cui et al., 2017).

In Arabidopsis accession Col-0, ETI conferred by the nuclear TNL pair RESISTANT TO RALSTONIA SOLANACEARUM1S (RRS1S)–RESISTANT TO PSEUDOMONAS SYRINGAE4 (RPS4) recognizing *Pseudomonas syringae* expressing effector AvrRps4 (*P. syringae* pv *tomato avrRps4*) has been used extensively to investigate *At*EDS1-*At*PAD4 signaling (Heidrich et al., 2011; Saucet et al., 2015). Col-0 *RRS1S-RPS4* ETI is associated with a weak cell death response (Heidrich et al., 2011), and to bolster basal immunity, *At*EDS1-*At*PAD4 complexes steer host transcriptional programs toward SA-induced defenses and away from SA-antagonizing jasmonic acid pathways (Zheng et al., 2012; Cui et al., 2018; Bhandari et al., 2019). This signaling involves positively charged amino acids at an *At*EDS1 EP domain surface lining a cavity formed by the EDS1-family heterodimer (Bhandari et al., 2019).

The function of EDS1-SAG101 complexes in TNL ETI was not determined, although *At*SAG101 but not *At*PAD4 was required for autoimmunity conditioned by the TNL pair CHILLING SENSITIVE3 (CHS3)–CONSTITUTIVE SHADE AVOIDANCE1 (CSA1) (Xu et al., 2015). In addition, TNL ETI but not basal immunity was retained in Arabidopsis accession Ws-2 expressing an *At*EDS1 variant (EDS1^{L262P}) that formed stable complexes with SAG101 but not PAD4 (Rietz et al., 2011). These data suggest that *At*EDS1-*At*PAD4 and *At*EDS1-*At*SAG101 heterodimers have distinctive roles in TNL ETI.

In this study, we examine EDS1-family sequence variation across seed plant lineages and test whether EDS1-PAD4 and EDS1-SAG101 complexes are functionally transferable between different plant groups. Despite high levels of conservation, we find barriers to EDS1 heterodimer functionality between plant lineages. By measuring resistance and cell death outputs of TNL signaling in Arabidopsis *N. benthamiana* ETI pathway mutants, we establish that *At*EDS1 and *At*SAG101 cooperate with *At*NRG1 in promoting cell death mediated by TNLs RRS1S-RPS4 and Recognition of XopQ1 (Roq1). We provide evidence that *At*PAD4 has a different immunity activity that strongly limits bacterial pathogen growth in Arabidopsis but is dispensable for TNL-triggered cell death and bacterial resistance in *N. benthamiana*. A structure-guided analysis of *At*EDS1 and *At*PAD4/*At*SAG101 variants indicates that decision-making between cell death and bacterial growth inhibition branches in TNL RRS1S-RPS4–mediated immunity is determined by distinctive features of the EDS1-SAG101 and EDS1-PAD4 complexes. Our data suggest that signaling machineries coevolved within plant species and clades for regulating downstream pathways in TNL-mediated immunity.

RESULTS

Dicotyledons from the Order Caryophyllales Lack Predicted SAG101 Orthologs

A previous study showed that EDS1 and PAD4 encoding genes are present in flowering plants (angiosperms; Wagner et al., 2013). In this study, we investigated the distribution of EDS1 family members using recent genomic information. Analysis of protein sequence orthogroups from genomes of 52 green plants shows that EDS1 and PAD4 are present in 46 seed plant species, including conifers (Figure 1; Supplemental Table 1; Supplemental Data Sets 1 to 3), suggesting that the EDS1 family arose in a common ancestor of gymno- and angiosperms. We did not detect EDS1-family orthologs in the aquatic monocot duckweed (*Spirodela polyrhiza*), consistent with the general loss of the *EDS1* family in flowering plants with an aquatic lifestyle (Baggs et al., 2019). As reported (Wagner et al., 2013), *At*SAG101 orthologs are absent from monocots and the basal eudicot *Aquilegia* and *Erythranthe guttata* (order Lamiales, formerly *Mimulus guttatus*). SAG101 was also not found in conifers or the eudicot species sugar beet (*Beta vulgaris*) from the order Caryophyllales (Supplemental Table 1). Reciprocal BLAST searches failed to identify putative *At*SAG101 orthologs in genomes and transcriptomes of nine additional Caryophyllales genomes (amaranth [*Amaranthus hypochondriacus*], quinoa [*Chenopodium quinoa*], spinach [*Spinacia oleracea*], and six species from the *Silene* genus). We concluded that loss of *SAG101* is likely common not only to monocots but also Caryophyllales eudicot species.

Next, we used 256 sequences of EDS1-family orthologs identified with OrthoMCL and additional BLAST searches to infer finely graded phylogenetic relationships (see "Methods"). On a maximum likelihood (ML) phylogenetic tree (Figure 1A), EDS1, PAD4, and SAG101 predicted proteins of flowering plants form clearly separated nodes. Conifer EDS1 and PAD4 belong to distinct clades that do not fall into the EDS1 and PAD4 of flowering plant groups. Therefore, functions of EDS1-family proteins might have diverged significantly between conifers and flowering plants. Conifer EDS1 further separated into two well-supported branches. Analyzed Solanaceae genomes (with the exception of pepper, [*Capsicum annuum*]) encode SAG101 proteins in two well-supported groups (A and B; Figure 1A), suggesting SAG101 diversification within Solanaceae. Because the EDS1 family tree topology is not known, we also performed a Bayesian inference of phylogeny (MrBayes phylotree; Supplemental Figure 1A), which supported conclusions drawn from the ML tree analysis (Figure 1A).

Although Brassicaceae, Caryophyllales, and Poaceae EDS1 and PAD4 form well-supported clades (Figure 1A; Supplemental Figure 1A), generally the EDS1 family does not provide sufficient resolution to separate other groups within flowering plants. This might be explained by conservation of the proteins and negative selection. Indeed, EDS1 sequences in Brassicaceae, Solanaceae, and Poaceae appear to have evolved mainly under purifying selection constraints (62.0–88.4% of sites; Supplemental Table 2). Mapping of evolutionary rates obtained with the refined EDS1, PAD4, and SAG101 phylogenetic trees (see "Methods") showed that slowly evolving (conserved) amino acids are present in the core lipase-like domain α/β-hydrolase folds and EP domain α-helical bundles likely to preserve structural stability but also on the partner EP domain surfaces lining the heterodimer cavity (Supplemental Figure 1B). Several conserved amino acids on this cavity surface of *At*EDS1 are essential for TNL-mediated immunity (Bhandari et al., 2019). The hydrophobic character of the LLIF α-helix in the *At*EDS1 lipase-like domain, which contacts hydrophobic pockets in corresponding *At*PAD4 and *At*SAG101 domains (Wagner et al., 2013), is also conserved across species (Supplemental Figure 1C). Although EDS1 sequences in three flowering plant families appear to have evolved mainly under purifying selection (Supplemental Table 2), analysis of evolutionary constraints indicated positive selection in Brassicaceae EDS1 sequences at five positions with multinucleotide mutations: R16, K215, Q223, R231, and K487 (Col-0 *At*EDS1 AT3G48090 coordinates; Supplemental Figures 1D and 1E; Supplemental Table 2). These amino acids are surface-exposed on the crystal structure of *At*EDS1, with the first four located in the lipase-like domain and K487 in the EP domain (Supplemental Figure 1E). Whether this variation has adaptive significance is unclear because an *At*EDS1^{K487R} variant retained TNL-mediated immunity function (Bhandari et al., 2019).

In summary, we find that EDS1 and PAD4 orthologs are present in conifers as well as flowering plants and form phylogenetically distinct sequence groups in these lineages. This finding suggests an origin of the EDS1 family in a common ancestor of seed plants. In addition, multiple species of the eudicot lineage Caryophyllales lack SAG101 orthologs, suggesting that loss of *SAG101* is not a sporadic event in the evolution of eudicots.

Interactions between EDS1-Family Proteins from Eudicot and Monocot Species

High conservation at the lipase-like EP domain interfaces of EDS1-SAG101 and EDS1-PAD4 (Supplemental Figure 1B) would be in line with heterodimer formation between partners in other species besides Arabidopsis and, potentially, interactions between EDS1 and PAD4 or SAG101 originating from different phylogenetic groups. Therefore, we tested EDS1-family protein interactions within and between representative species of eudicot (Brassicaeae, Solanaceae) and monocot (Poaceae) families. In yeast two hybrid (Y2H) assays, EDS1 and PAD4 from the same species or family formed a complex (Figure 1B). Notably, tomato (*Solanum lycopersicum*) EDS1 also interacted with *At*PAD4 and barley (*Hordeum vulgare*) and *Brachypodium distachyon* PAD4 proteins (Figure 1B). By contrast, *At*EDS1 and monocot *Hv*EDS1 or *Bd*EDS1 did not interact with either *Sl*PAD4 or potato (*Solanum tuberosum*) *St*PAD4. These data show that EDS1 and PAD4 partners within species that are distant from Arabidopsis also interact physically and there are some between-clade associations.

We selected Arabidopsis, tomato, and barley EDS1-PAD4 combinations for in planta coimmunoprecipitation (co-IP) assays of epitope-tagged proteins transiently expressed after *Agrobacterium tumefaciens* (agroinfiltration) of *N. benthamiana* leaves. As expected, *At*PAD4-yellow fluorescent protein (YFP) immunoprecipitated with coexpressed *At*EDS1-FLAG. This interaction was strongly reduced when the *At*EDS1 LLIF N-terminal heterodimer contact was mutated (Figure 1C; Wagner et al., 2013).
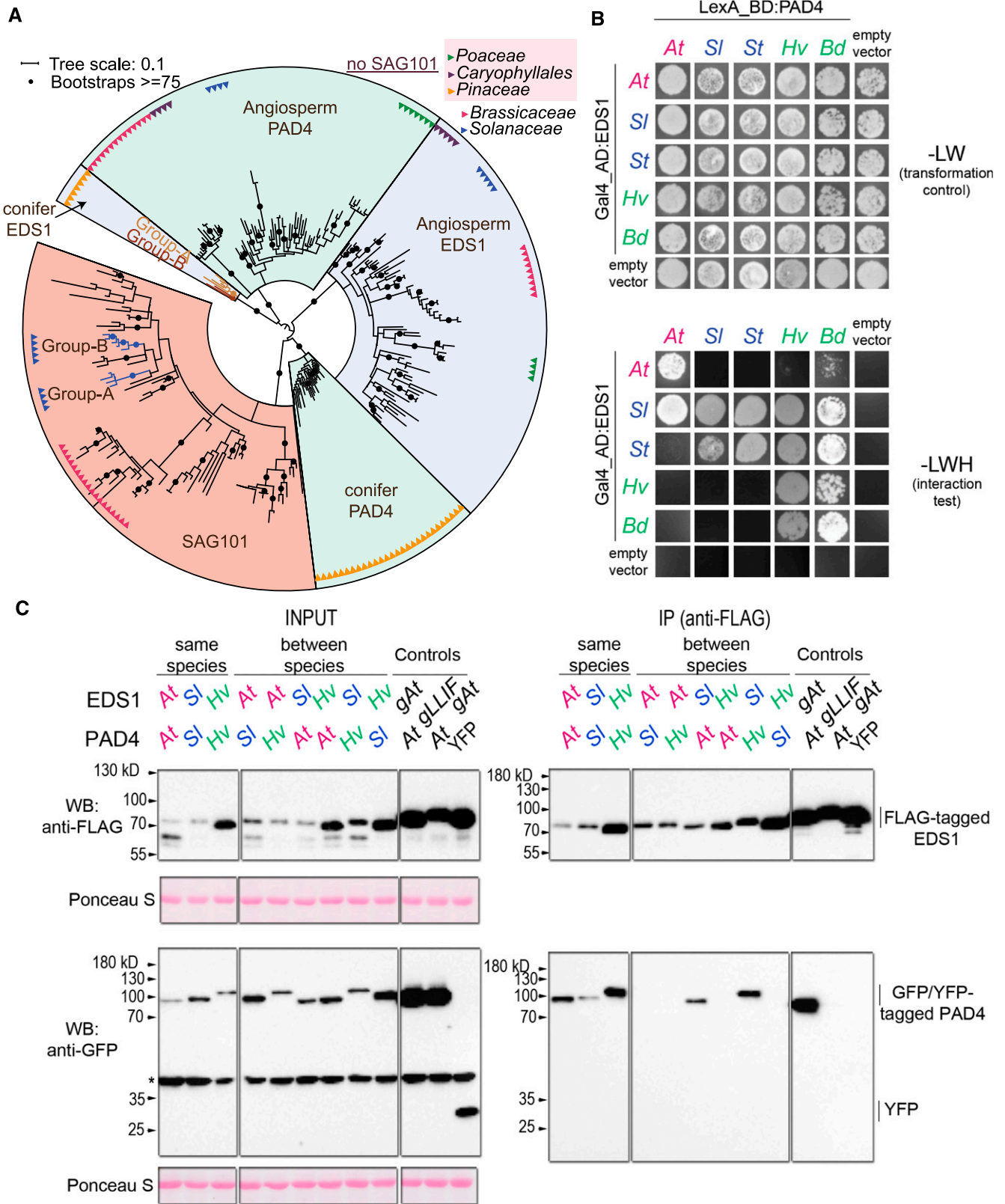
Figure 1. Phylogeny Of EDS1-Family Proteins in Seed Plants and Conservation of EDS1-PAD4 Interactions in Angiosperms.

In accordance with the Y2H data, YFP-SlPAD4 and YFP-HvPAD4 immunoprecipitated with FLAG-EDS1 from the same species (SlEDS1 and HvEDS1). In addition, FLAG-SlEDS1 interacted with YFP-AtPAD4 and YFP-HvPAD4, but FLAG-AtEDS1 did not interact with either YFP-SlPAD4 or YFP-HvPAD4 (Figure 1C). Similarly, FLAG-HvEDS1 failed to interact with YFP-AtPAD4 or YFP-SlPAD4 (Figure 1C). Therefore, EDS1 and PAD4 from the same eudicot or monocot species form stable complexes in planta like AtEDS1-AtPAD4, suggesting that EDS1-PAD4 heterodimer formation is a conserved feature across angiosperms. In Y2H and in planta, between-clade complex formation is not universal, indicating that barriers exist for certain EDS1-PAD4 partner interactions between distant lineages.

We also tested in *N. benthamiana* transient assays whether SlEDS1 or AtEDS1 can form complexes with SAG101 proteins from Solanaceae (*N. benthamiana*) and Arabidopsis. Tomato has two *SAG101* genes that fall respectively into Solanaceae SAG101 groups A and B (Figure 1A; Supplemental Figure 1A) and are most sequence-related to NbSAG101a and NbSAG101b (81.52% and 72.44% sequence identity; Supplemental Data Set 4). As expected, AtEDS1-FLAG interacted with AtSAG101-YFP in IP assays (Supplemental Figure 2A). In addition, FLAG-SlEDS1 interacted with NbSAG101a-green fluorescent protein and NbSAG101b-GFP, consistent with the close phylogenetic relationship between cultivated tomato and *N. benthamiana*. Notably, FLAG-SlEDS1 immunoprecipitated AtSAG101-YFP, but AtEDS1-FLAG did not immunoprecipitate NbSAG101a or NbSAG101b (Supplemental Figure 2A), similar to the AtEDS1/SlPAD4 combinations (Figures 1B and 1C). As shown previously (Feys et al., 2005), AtSAG101-YFP localized to the nucleus, whereas NbSAG101a-GFP and NbSAG101b-GFP had a nucleocytoplasmic distribution in *N. benthamiana* (Supplemental Figure 2B). Together, the data suggest that EDS1-partner interactions are conserved across angiosperms, but there are some restrictions to protein interactions between different taxonomic groups.

Tomato EDS1-PAD4 Is Functional in Arabidopsis *TNL RPP4* and *RRS1S-RPS4* Immunity

The data above show that tomato EDS1 (SlEDS1) forms a stable complex with tomato and Arabidopsis PAD4 proteins (Figures 1B and 1C). Because heterodimerization of EDS1 with PAD4 or

SAG101 is essential for TNL signaling in Arabidopsis (Rietz et al., 2011; Wagner et al., 2013), we tested whether SlEDS1-SlPAD4 signal together or with their respective AtEDS1 and AtPAD4 partners in Arabidopsis TNL-mediated immunity (Figure 2). For this, four EDS1-PAD4 coexpression constructs (AtEDS1-AtPAD4, SlEDS1-SlPAD4, SlEDS1-AtPAD4, AtEDS1-SlPAD4; Figure 2A) were transformed into a triple mutant line, *eds1-2 pad4-1 sag101-3*, in accession Col-0. Arabidopsis or tomato EDS1 and PAD4 coding sequences were fused to N-terminal FLAG and YFP tags, respectively. Expression of the genes was driven by the Arabidopsis *EDS1* and *PAD4* promoters (Gantner et al., 2019). Three independent transgenic lines expressing the tagged proteins (Figure 2A) were selected and spray-inoculated with the downy mildew pathogen *Hyaloperonospora arabidopsidis* isolate Emwa1, which is recognized in Col-0 by the TNL receptor RPP4 (Van Der Biezen et al., 2002; Asai et al., 2018). Pathogen spores were quantified on leaves at 7 d after inoculation (DAI).

Col-0 expressing StrepII-3xHA-YFP was resistant to *H. arabidopsidis* Emwa1, whereas *eds1-2 pad4-1 sag101-1* and accession Ws-2 (which lacks *RPP4*; Holub, 1994) were susceptible (Figure 2B). The AtEDS1-AtPAD4 pair fully restored *H. arabidopsidis* resistance in *eds1-2 pad4-1 sag101-3* (Figure 2B), consistent with an EDS1-PAD4 heterodimer being necessary for TNL-mediated immunity in Arabidopsis (Glazebrook et al., 1997; Feys et al., 2001; Rietz et al., 2011; Wagner et al., 2013). The SlEDS1-SlPAD4 pair also conferred full *RPP4* immunity (Figure 2B). Thus, SlEDS1-SlPAD4 is functionally transferable from tomato to Arabidopsis. By contrast, between-species EDS1-PAD4 combinations AtEDS1-SlPAD4 and SlEDS1-AtPAD4 did not fully prevent *H. arabidopsidis* sporulation. Although no *RPP4* resistance was detected in Arabidopsis lines expressing AtEDS1-SlPAD4 (which did not interact in Y2H and IP assays; Figures 1B and 1C), there was a partial resistance response in plants expressing SlEDS1-AtPAD4 (Figure 2B), which did interact (Figures 1B and 1C). We also tested functionality of the EDS1-PAD4 combinations in resistance mediated by the TNL pair RRS1S-RPS4. Again, AtEDS1-AtPAD4 and SlEDS1-SlPAD4 restricted *P. s. tomato avrRps4* growth fully, whereas SlEDS1-AtPAD4 were partially functional and AtEDS1-SlPAD4 failed to confer TNL *RRS1S-RPS4* resistance (Figure 2C). We concluded that the between-clade SlEDS1-AtPAD4 combination likely retains some TNL resistance signaling function because it forms a heterodimer (Figures 1B and 1C), but incompatibility with Arabidopsis factors

---

Figure 1. (continued).

(A) ML tree of 256 sequences from predicted EDS1-family proteins. Branches with Felsenstein bootstrap support values ≥75 are given as black dots. EDS1, PAD4, and SAG101 orthologs form separate groups. Solanaceae SAG101 falls into two groups: A and B. Similarly, conifers have two EDS1 groups labeled A and B.

(B) A yeast two hybrid assay testing interactions between EDS1 and PAD4 from Arabidopsis (*At*), tomato (*Sl*), potato (*St*), barley (*Hv*), and *B. distachyon* (*Bd*). –LW indicates dropout selection medium without Leu and Trp. –LWH indicates medium without Leu, Trp, and His. Each combination shown was tested in two to four independent experiments with similar results.

(C) Protein gel blot analysis with anti-FLAG or anti-GFP antibodies showing proteins before (INPUT) and after immunoprecipitation (IP) assay to test in planta interactions between Arabidopsis, tomato (*Sl*), and barley (*Hv*) EDS1 and PAD4 orthologs, as indicated. Proteins were transiently coexpressed in *N. benthamiana*. IPs using Arabidopsis (*At*) pEDS1:gEDS1-3xFLAG (gAt) or pEDS1:gEDS1_LLIF/AAAA-3xFLAG (gLLIF) with Arabidopsis (*At*) 35S:PAD4-YFP served as positive and negative controls, respectively. Ponceau S staining of the membrane shows equal loading of input samples. Combinations were tested in four independent experiments with the exception of FLAG-SlEDS1/YFP-HvPAD4 and FLAG-HvEDS1/YFP-SlPAD4, which were repeated twice. *Bands likely resulting from unspecific antibody binding.
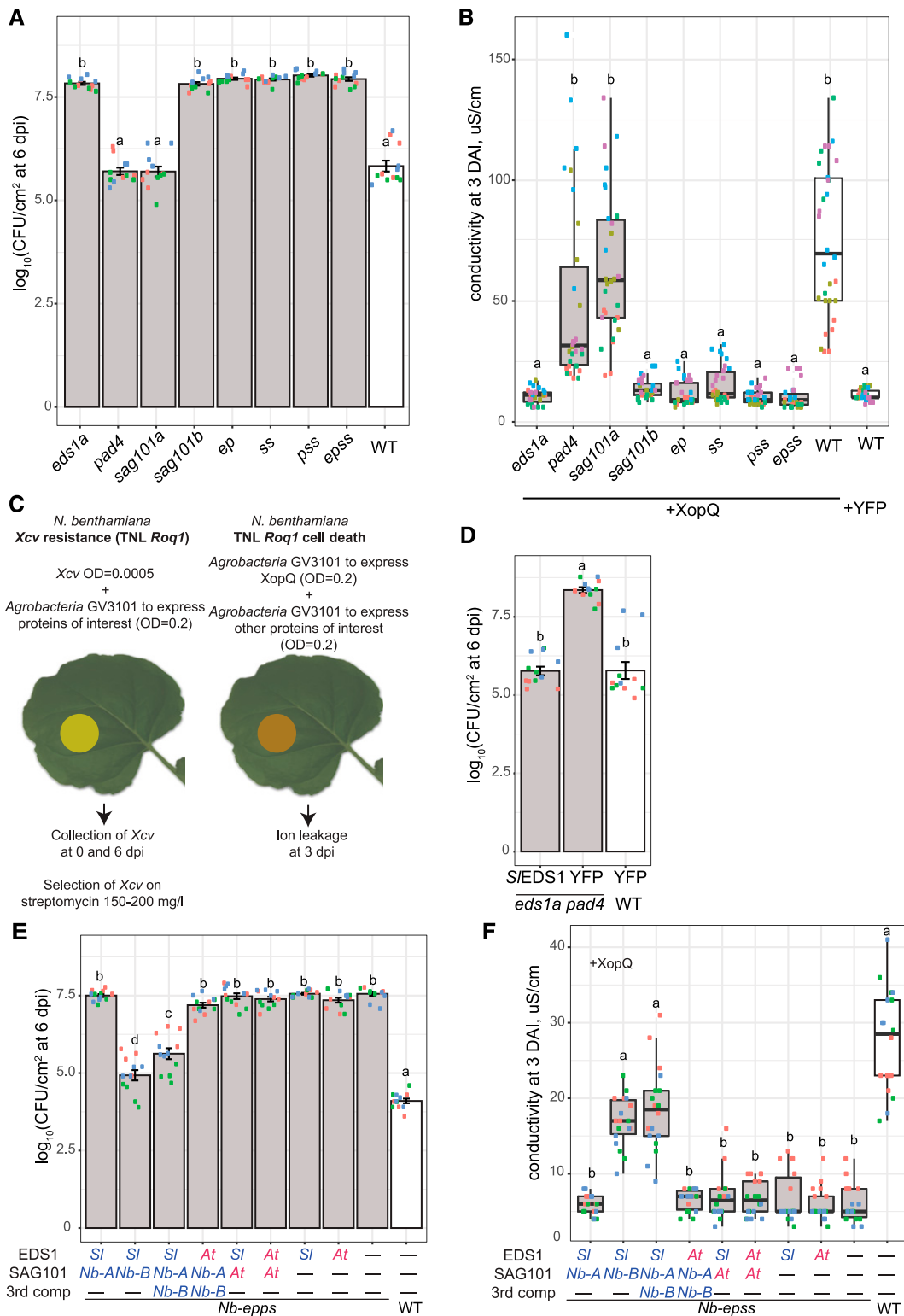
Figure 2. A Tomato EDS1-PAD4 Pair Functions in Arabidopsis TNL RPP4 and RRS1S-RPS4–Dependent Iimmunity.

(A) At left, schematic representation of a Golden Gate assembled fragment to express coding sequences of Arabidopsis and tomato (*Sl*) EDS1 and PAD4 under the control of corresponding Arabidopsis promoters in Arabidopsis Col *eds1-2 pad4-1 sag101-3*. At right, protein gel blot analysis of FLAG-EDS1 and GFP-PAD4 proteins in 5-week-old Arabidopsis independent T4 transgenic lines, as indicated. Ponceau S staining of the membrane served as a loading control. The analysis was performed twice with similar results.

(B) A TNL (RPP4) resistance assay in the T3 independent transgenic lines. *H. arabidopsidis* Emwa1 conidiospores on leaves were quantified at 7 DAI. An Arabidopsis Col StrepII-3xHA-YFP (Col YFP, resistant), Ws-2 (*rpp4*, susceptible) and nontransformed Col *eds1-2 pad4-1 sag101-1* (*eps*, susceptible) served as controls. Data from three independent experiments (biological replicates) are represented in a box plot with dots in the same color corresponding to technical replicates (individual normalized spore counts) from one independent experiment. Genotypes sharing letters above box whiskers on the plot do not show statistically significant differences (Nemenyi test, $\alpha = 0.01$, $n = 15$).

(C) A TNL (RRS1S-RPS4) resistance assay in T4 independent transgenic lines, as shown at right in **(A)**. *P. s. tomato* DC3000 *avrRps4* was syringe infiltrated (OD$_{600}$ = 0.0005) into leaves of 5-week-old plants, and titers were determined at 3 DAI. Arabidopsis Col StrepII-3xHA-YFP (Col YFP, resistant), Col *eds1-2 pad4-1 sag101-1* (*eps*, susceptible) served as controls. Because some transgenic lines were still segregating, only plants that survived BASTA spraying at 2 weeks after germination were used in the assay. Data from three independent experiments (biological replicates) are represented in a bar plot with dots in the same color corresponding to technical replicates (individual dilutions) from one independent experiment. Genotypes sharing letters above box whiskers on the plot do not show statistically significant differences (Tukey HSD test, $\alpha = 0.001$, $n = 15$).

might prevent it from functioning fully in Arabidopsis TNL signaling.

*Sl*EDS1 Functions with *Nb*SAG101b in *N. benthamiana* TNL Roq1-Mediated Immunity

To explore further whether EDS1 family members are functionally transferable between eudicot species for TNL-mediated immunity, we exploited the *N. benthamiana* TNL Roq1 resistance system (Figure 3). Roq1 recognizes the type 3–secreted effector XopQ delivered from leaf-infecting *Xanthomonas campestris* pv *vesicatoria* bacteria (Adlung et al., 2016; Schultink et al., 2017). This recognition induces *NbEDS1a*-dependent cell death and resistance to pathogen growth (Adlung et al., 2016; Schultink et al., 2017; Qi et al., 2018). To measure requirements for *PAD4* and *SAG101* in *N. benthamiana* TNL Roq1 signaling, we generated

Figure 3. Tomato or *N. benthamiana* EDS1 Signal With *Nb*SAG101b in TNL Roq1-Dependent Resistance and Cell Death.

(A) *X. c. vesicatoria* growth assay in *N. benthamiana EDS1*-family mutants at 6 DAI. *X. c. vesicatoria* was syringe infiltrated at $OD_{600} = 0.0005$. Different letter codes above bars show that differences between genotypes are statistically significant (Tukey HSD, $\alpha = 0.001$, $n = 12$ from three independent experiments

an *N. benthamiana* quadruple knockout mutant of EDS1-family genes (denoted *Nb-epss*; *EDS1a*, *PAD4*, *SAG101a*, and *SAG101b*) by crossing *Nb-eds1a* with *Nb-pad4 sag101a sag101b* (Ordon et al., 2017; Gantner et al., 2019). The *Nb-epss* mutant was tested alongside single (*eds1a*, *pad4*, *sag101a*, *sag101b*), double (*eds1a pad4*, *sag101a sag101b*), and triple (*Nb-pad4 sag101a sag101b*) mutants for defects in XopQ-triggered resistance to *X. c. vesicatoria* growth (Figure 3A) and host cell death, measured as ion leakage after Agrobacteria-mediated transient expression of XopQ-myc (Figure 3B). The *pad4* and *sag101a* single mutants displayed wild-type *X. c. vesicatoria* resistance and host cell death responses, indicating that *PAD4* and *SAG101a* are dispensable for TNL Roq1-mediated immunity. By contrast, *eds1a* and *sag101b* mutant lines supported high *X. c. vesicatoria* titers (2.0-2.5 $\log_{10}$ relative to the wild type; Figure 3A) and did not develop XopQ-triggered cell death (Figure 3B). These data show that *NbEDS1a* and *NbSAG101b* confer Roq1-mediated *X. c. vesicatoria* resistance and host cell death. Similarity between *X. c. vesicatoria* titers in the *epss* and *eds1a* mutants (Figure 3A) suggest that *NbEDS1a* is not able to recruit *NbPAD4*, and *NbSAG101* forms redundantly for *N. benthamiana* TNL (Roq1) immunity.

To further test the differential requirement for *NbPAD4* and *NbSAG101* in Roq1 signaling, we performed complementation assays. In these assays, Agrobacteria-mediated transient expression of proteins in *N. benthamiana*, in combination with simultaneous *X. c. vesicatoria* infiltration or XopQ-myc agroinfiltration of leaf sectors, was used to monitor TNL Roq1-dependent resistance and cell death outputs (Figure 3C). We initially assessed whether Agrobacteria infiltration interferes with wild-type *N. benthamiana* resistance to *X. c. vesicatoria* (Supplemental Figure 3A). Streptomycin (at 150–200 mg/L) allowed selective growth on agar plates of *X. c. vesicatoria* but not *A. tumefaciens* strain GV3101 bacteria extracted from leaves. *A. tumefaciens* infiltrated at two densities (OD$_{600}$ 0.1 and 0.4, strain to express YFP) did not affect *X. c. vesicatoria* growth in susceptible *Nbeds1a* but further reduced *X. c. vesicatoria* proliferation in resistant wild-type

N. benthamiana leaves (Supplemental Figure 3A). We took the 2.5 to 3 $\log_{10}$ difference in *X. c. vesicatoria* titers between the wild type and *Nbeds1a* on agroinfiltration as a measure of *EDS1*-dependent *TNL* resistance to *X. c. vesicatoria* growth. Susceptibility to *X. c. vesicatoria* in the *Nbeds1a pad4* double mutant was converted to full resistance after Agrobacteria-mediated expression of FLAG-*Sl*EDS1 but not YFP (Figure 3D), further validating that PAD4 is not essential for *Roq1*-triggered immunity. This result also shows that FLAG-*Sl*EDS1 is functional in *N. benthamiana Roq1*-dependent *X. c. vesicatoria* growth restriction.

Transient coexpression of *Nb*SAG101b-GFP but not *Nb*SAG101a-GFP with functional FLAG-*Sl*EDS1 (Figure 3D) restored resistance to *X. c. vesicatoria* growth in *Nb-epss*, although not completely to the level of wild-type *N. benthamiana* (Figure 3E). A difference in the degree to which *Sl*EDS1 confers resistance to *X. c. vesicatoria* between *Nbeds1a pad4* (Figure 3D) and *Nb-epss* (Figure 3E) might be due to delayed accumulation of *Nb*SAG101b in *Nb-epss* (in which the protein is expressed transiently) compared with native *Nb*SAG101b in *Nbeds1a pad4*. In Arabidopsis, NLR resistance against bacteria depends on timely host transcription reprogramming (Mine et al., 2018; Bhandari et al., 2019). In addition, FLAG-*Sl*EDS1 functioned with *Nb*SAG101b-GFP, but not *Nb*SAG101a-GFP, in conferring *Roq1*-dependent cell death, as quantified in a leaf disc ion leakage assay at 3 DAI of XopQ-myc with the protein combinations (Figure 3F). Immunoblot analysis at 2 DAI showed that *Nb*SAG101a-GFP and *Nb*SAG101b-GFP accumulated to similar levels in these assays (Supplemental Figure 3B). We concluded that *Nb*SAG101b, but not *Nb*SAG101a or *Nb*PAD4, functions together with *Sl*EDS1 or endogenous *Nb*EDS1a in *N. benthamiana* Roq1-mediated immunity.

*At*EDS1 with *At*SAG101 Does Not Restore TNL *Roq1*-Dependent Signaling in *Nb-epss* Leaves

In *N. benthamiana* cell death and resistance assays, we tested whether *At*EDS1-*At*SAG101 or the heterologous interacting

---

Figure 3. (continued).

used as biological replicates). Error bars represent ±sem. ep = *eds1a pad4*, ss = *sag101a sag101b*, pss = *pad4 sag101a sag101b*, epss = *eds1a pad4 sag101a sag101b*. CFU, colony forming units. WT, wild type.

(B) Ion leakage assay as a measure of Roq1-mediated cell death in *N. benthamiana EDS1*-family mutants at 3 days after infiltration (DAI) of Agrobacteria to express XopQ-myc. Genotypes with the same letter code do not show statistically significant differences in the extent ion leakage (Nemenyi test, $\alpha = 0.01$, $n = 30$ from five independent experiments used as biological replicates). WT, wild type.

(C) Schematic showing *N. benthamiana* transient complementation assays to test protein functionalities in Roq1-dependent immunity at the level of *X. c. vesicatoria* growth inhibition and XopQ triggered cell death (see Methods for details).

(D) *X. c. vesicatoria* growth assay in *Nb eds1a pad4* plants with transiently expressed *pAtEDS1:FLAG-SlEDS1*. Overlapping letter codes above bars show that differences between genotypes are not statistically significant (Tukey HSD, $\alpha = 0.001$, $n = 12$ from three independent experiments used as biological replicates). Error bars represent ±sem. WT, wild type.

(E) *X. c. vesicatoria* growth assay in *N. benthamiana* eds1a pad4 sag101a sag101b (*Nb*-epss) combined with transient expression of pAtEDS1:FLAG-SlEDS1 (*Sl*), 35S:NbSAG101a-GFP (*Nb*-A), 35S:NbSAG101b-GFP (*Nb*-B), pAtEDS1:AtEDS1-YFP (*At*), 35S:AtSAG101-YFP (*At*), or 35S:YFP ("-"), as indicated. Dots of the same color in box plots represent technical replicates (individual extractions of bacteria) in one of three independent experiments (biological replicates). The same letters above bars indicate that differences in means are not statistically significant between genotypes (Tukey HSD, $\alpha = 0.001$, $n = 12$). Error bars represent ±sem. WT, wild type.

(F) Ion leakage assay as a measure of Roq1-mediated cell death triggered by XopQ-myc in *Nb-epss* plant after transient expression of the same protein combinations as in **(E)**. Cell death was measured as an increase in conductivity relative to a YFP-negative control (all "-" in sample description). The experiment was repeated three times with six leaf discs used as technical replicates (same colored dots correspond to replicates in each independent experiment used a biological replicate). Statistical significance of differences between samples was assessed using a Nemenyi test ($\alpha = 0.01$, $n = 18$). WT, wild type.

SlEDS1-AtSAG101 and noninteracting AtEDS1-NbSAG101b pairs (Supplemental Figure 2A) could substitute for endogenous NbEDS1a and NbSAG101b in Roq1 immunity. None of these EDS1-SAG101 combinations mediated Roq1-dependent restriction of X. c. vesicatoria bacterial growth at 6 DAI (Figure 3E) or XopQ triggered cell death at 3 DAI (Figure 3F) in Nb-epss. All tagged proteins accumulated in these assays, as measured on immunoblots at 2 DAI (Supplemental Figure 3B). Consequently, AtEDS1 and AtSAG101, as a homologous pair or together with functional NbSAG101b and SlEDS1, do not confer Roq1-dependent signaling. We concluded that the Arabidopsis EDS1-SAG101 heterodimer is inactive or insufficient for signaling in TNL Roq1-mediated immunity in N. benthamiana.

AtEDS1 and AtSAG101 with AtNRG1.1 or AtNRG1.2 Rescue XopQ-Triggered Cell Death in Nb-epss

SAG101 and NRG1 were reported to be absent from monocots and several dicot species (Aquilegia coerulea, E. guttata; Collier et al., 2011; Wagner et al., 2013). Because we additionally did not find SAG101 in conifers and Caryophyllales (Supplemental Table 1), we searched for NRG1 in these species. Manual reciprocal BLAST searches in nine genomes and transcriptomes of Caryophyllales (amaranth, quinoa, spinach, and six Silene species) failed to identify NRG1 orthologs. Similarly, an OrthoMCL-derived NRG1 orthogroup did not contain conifer sequences, whereas ADR1 orthologs were detected in the examined conifer and Caryophyllales species (Supplemental Table 1). The strong SAG101 and NRG1 co-occurrence signature combined with Roq1 dependency on NbSAG101b (Figure 3) and NbNRG1 (Qi et al., 2018) in N. benthamiana prompted us to test whether AtNRG1.1 or AtNRG1.2 expressed with AtEDS1-AtSAG101 confer X. c. vesicatoria resistance and/or XopQ-triggered cell death in N. benthamiana.

Previously, tagged NbNRG1, AtNRG1.1, and AtNRG1.2 forms or their corresponding CC domains were shown to elicit cell death on agroinfiltration of N. benthamiana leaves (Peart et al., 2005; Collier et al., 2011; Wróblewski et al., 2018; Wu et al., 2019). Using the quantitative ion leakage assay, we tested whether transiently expressed AtNRG1.1 or AtNRG1.2 controlled by a 35S promoter induce cell death in N. benthamiana. We also examined whether their cell death activity is affected by N- or C-terminal StrepII-HA (SH) or enhanced GFP (eGFP) epitope tags and the presence or absence of functional NbEDS1a. The cell death response in both backgrounds at 3 DAI was strong for N- and C-terminal eGFP-tagged AtNRG1.2 and weak for SH-tagged AtNRG1.2 (Supplemental Figure 4A). By contrast, N- and C-terminal eGFP- or SH-tagged AtNRG1.1, as well as nontagged AtNRG1.1 or AtNRG1.2 forms, did not induce cell death in these two N. benthamiana genotypes (Supplemental Figure 4A). Immunoblot analysis of the expressed proteins at 2 DAI showed that AtNRG1.1-eGFP and AtNRG1.2-eGFP accumulated to similar levels as YFP in both backgrounds (Supplemental Figure 4B). All eGFP-tagged AtNRG1.1 and AtNRG1.2 forms were detected in the cytoplasm (Supplemental Figure 4C). The data suggest that tagged AtNRG1.2, but not AtNRG1.1, induces cell death independent of NbEDS1a, NbPAD4 and XopQ activation of TNL Roq1 in N. benthamiana. To avoid possible AtNRG1 autonomous

cell death activity, we used the AtNRG1.1-SH variant in subsequent TNL Roq1 immunity assays, because it was clearly detectable (as two bands) on immunoblots (Supplemental Figure 4B) and did not elicit cell death in TNL-nontriggered N. benthamiana leaves, similar to the untagged AtNRG1.1 and AtNRG1.2 proteins (Supplemental Figure 4A). These results emphasize a need to consider the effect of tags in analysis of NRG1 molecular functions.

Agrobacteria-mediated transient expression of nontagged AtNRG1.1, nontagged AtNRG1.2, or AtNRG1.1-SH together with AtEDS1-YFP and AtSAG101-SH produced cell death in Nb-epss leaves that was as strong as the wild-type N. benthamiana response to XopQ-myc infiltration (Figure 4A). Without XopQ-myc, none of the three AtEDS1-AtSAG101-AtNRG1 combinations produced ion leakage above the negative control (YFP alone) at 3 DAI (Figure 4A), indicating that the cell death response is XopQ recognition dependent. Immunoblot analysis at 2 DAI indicated that AtNRG1.1-SH, AtEDS1-YFP, AtSAG101-SH proteins accumulated to similar levels in XopQ-myc treated and nontreated leaf extracts (Supplemental Figure 5A). These data show that AtEDS1 and AtSAG101 coexpressed with either AtNRG1.1 or AtNRG1.2 can restore XopQ/Roq1-triggered cell death in Nb-epss leaves. When AtSAG101-SH was substituted by SH-AtPAD4 in the assays (Supplemental Figure 5B), this did not restore Roq1-mediated cell death (Figure 4B). We concluded that AtEDS1-AtSAG101-AtNRG1, but not AtEDS1-AtPAD4-AtNRG1, reconstitute a TNL cell death signal transduction module in this Solanaceae species. Because AtEDS1 and AtSAG101 failed to function with endogenous NbNRG1 in triggering Roq1-dependent cell death (Figure 3E), there appears to be a requirement for molecular compatibility between these immunity components within species or clades.

AtEDS1-AtPAD4 with AtADR1-L2 Do Not Confer Roq1-Dependent Cell Death or Bacterial Resistance

In Arabidopsis, PAD4 and SAG101 were suggested to cooperate genetically with ADR1- or NRG1-family helper NLRs in TNL autoimmunity, respectively (Wu et al., 2019). We hypothesized that AtPAD4 requires a matching AtADR1 protein to function in N. benthamiana. AtADR1-L2-HA complemented resistance and cell death defects in an Arabidopsis ADR1-family null mutant (Bonardi et al., 2011), so we used AtADR1-L2 with a short C-terminal SH tag in the N. benthamiana Roq1-dependent cell death complementation assays. Consistent with experiments in Figures 4A and 4B, coexpression of AtEDS1-FLAG, AtSAG101-FLAG, and AtNRG1.1-SH induced ion leakage at 3 DAI in the presence of XopQ-myc (Figure 4C), showing that AtEDS1 and AtSAG101 activity in Roq1-dependent cell death is tag independent. A combination of AtEDS1-FLAG, AtPAD4-FLAG and AtADR1-L2-SH did not lead to XopQ-triggered cell death (Figure 4C). Immunoblot analysis at 2 DAI showed that AtSAG101-FLAG and AtPAD4-FLAG were expressed at similar levels, as were AtNRG1.1-SH and AtADR1-L2-SH (Supplemental Figure 5C). Next we tested whether AtEDS1-AtSAG101-AtNRG1.1 or AtEDS1-AtPAD4-AtADR1-L2 signal in Roq1-dependent resistance to X. c. vesicatoria in Nb-epss leaves. The combination of AtEDS1-FLAG, AtSAG101-FLAG, and AtNRG1.1-SH
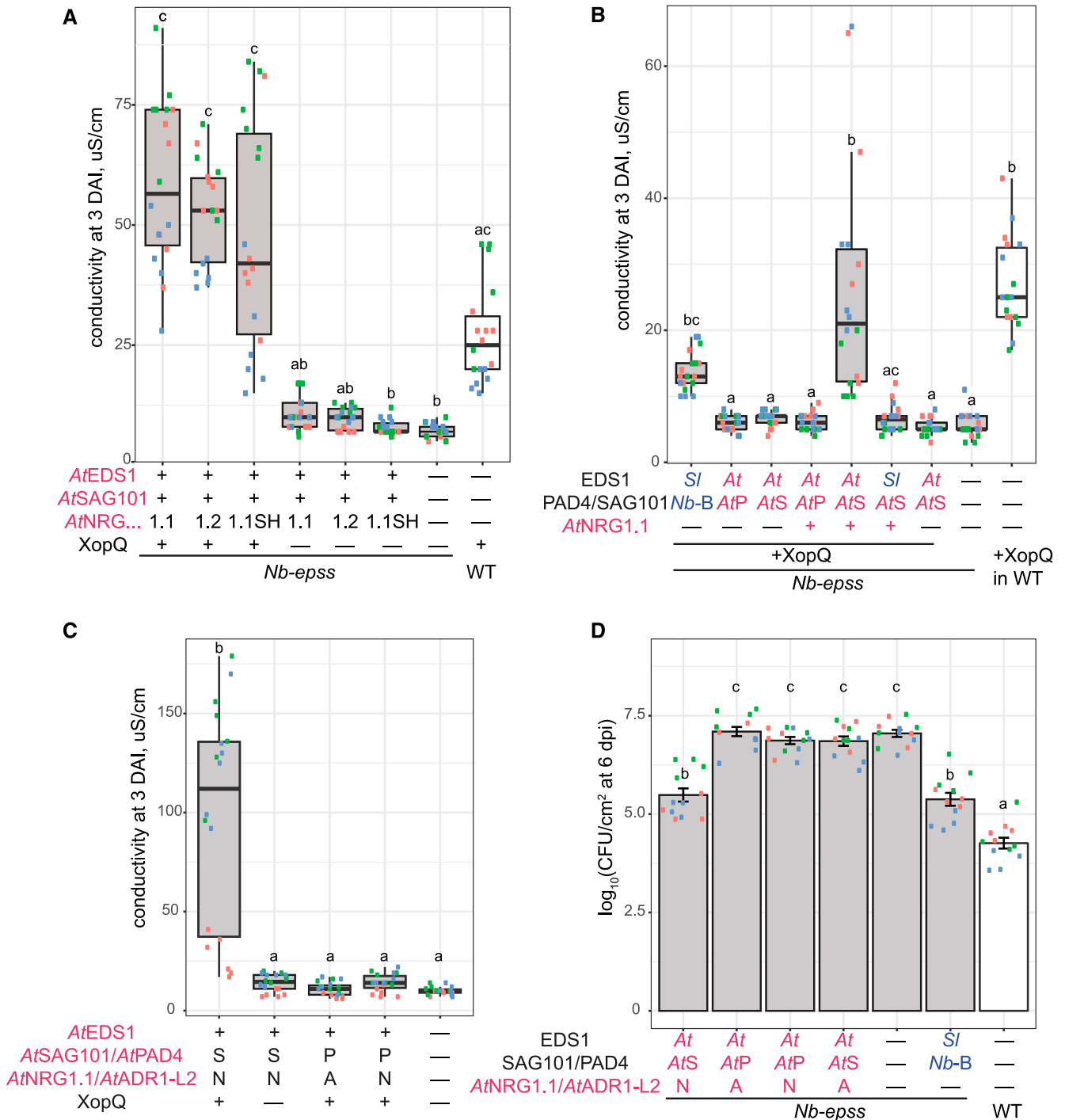
Figure 4. An *At*EDS1-*At*SAG101-*At*NRG1.1 Module Rescues Roq1-Dependent Cell Death and Resistance in *N. benthamiana*.

(A) Ion leakage assay in *N. benthamiana* wild type (WT;white) and *eds1a pad4 sag101a sag101b* (*Nb-epss*, gray) plants transiently expressing combinations of Arabidopsis EDS1-YFP, SAG101-SH, untagged or C-terminally SH-tagged NRG1.1 or NRG1.2 proteins in the presence of *X. c. vesicatoria* effector XopQ-myc. "−" in the sample description refers to YFP. Conductivity measurements were performed at 3 d after Agrobacteria infiltration. The experiment was repeated three times (dots of the same color represent six technical replicates [leaf discs] from one independent experiment [biological replicate]). Shared letters above the box whiskers between samples indicate that differences are not statistically significant (using a Nemenyi test, α = 0.01, *n* = 18).
(B) Ion leakage assay in *N. benthamiana* wild type (WT; white) and *Nb-epss* (gray) plants transiently expressing combinations of FLAG-*Sl*EDS1, *At*EDS1-FLAG with SH-*At*PAD4 (*At*P) or *At*SAG101-SH (*At*S) and *At*NRG1.1-SH, as indicated, in the presence of XopQ-myc. "−" in sample descriptions indicates

restored resistance to the same extent as an *Sl*EDS1-*Nb*SAG101b control pair (Figure 4D). By contrast, coexpression of *At*EDS1-FLAG and *At*PAD4-FLAG with *At*ADR1-L2-SH did not lead to bacterial resistance (Figure 4D).

These data show that *At*EDS1-*At*SAG101-*At*NRG1.1 can confer cell death and bacterial resistance initiated by TNL Roq1 in the *N. benthamiana* complementation assay. They further show that native *Nb*EDS1a-*Nb*PAD4 or the *trans*-clade *At*EDS1-*At*PAD4 pair (with or without *At*ADR1-L2) do not contribute to Roq1-mediated cell death and bacterial resistance. This finding contrasts with important roles of *Sl*EDS1-*Sl*PAD4 and *At*EDS1-*At*PAD4 partners in Arabidopsis TNL (*RPP4* and *RRS1S-RPS4*) immunity (Figure 2).

An EP Domain α-Helical Coil Surface on *At*SAG101 Confers *Roq1*-Dependent Cell Death

The above data suggest that the *At*EDS1-*At*SAG101 heterodimer has a distinctive feature that is not shared by *At*EDS1-*At*PAD4 (Supplemental Figure 1B; Wagner et al., 2013), which enables cooperation with *At*NRG1.1 in XopQ/*Roq1*-dependent cell death in *Nb-epss* plants (Figures 4A and 4C). Several *At*EDS1 EP domain residues lining a cavity formed by the heterodimer are essential for *At*EDS1-*At*PAD4 TNL-mediated immunity signaling in Arabidopsis (Bhandari et al., 2019). Examining EDS1-PAD4 and EDS1-SAG101 evolutionary rate variation across seed plants (Supplemental Figure 1B) highlighted conserved residues on a prominent α-helical coil of *At*PAD4 and *At*SAG101 that spans the length of the EP domain cavity and, at its base, creates contacts with the *At*EDS1 EP domain (Supplemental Figure 1B; Wagner et al., 2013). Therefore, we generated four *At*PAD4-*At*SAG101 chimeric proteins (chimeras 1 to 4) with decreasing *At*SAG101 contributions to this central EP domain α-helical coil (Figure 5A, SAG101 shown in pink). All four *At*PAD4-*At*SAG101 chimeras contained the complete *At*PAD4 N-terminal lipase-like domain (Figure 5A, green). In *Nb-epss* cell death assays, chimeras 1 to 4 fused N-terminally to a StrepII-YFP tag exhibited a nucleocyto-plasmic localization, like YFP-*At*PAD4 (Supplemental Figure 6). We tested the chimeras in the *Nb-epss* TNL *Roq1*-dependent cell death reconstitution assay, as previously, with coexpressed *At*EDS1-YFP, *At*NRG1.1-SH, and XopQ-myc. Chimeras 1 and 2 mediated XopQ-dependent cell death, whereas chimeras 3 and 4 were inactive in quantitative ion leakage assays and macro-scopically at 3 DAI (Figures 5B and 5C). All chimeras accumulated

to similar levels but less well than YFP-*At*PAD4 or *At*SAG101-YFP full-length proteins at 2 DAI (Supplemental Figure 5D). Comparing the sequences of functional and nonfunctional chimeras 2 and 3 allowed us to delineate an *At*SAG101 α-helical coil patch required for cell death reconstitution to between amino acids 289 and 308 (Supplemental Figure 5E). These results suggest that a discrete region of the *At*SAG101 EP domain is necessary for conferring reconstituted *Roq1*-dependent cell death.

Reconstituted Roq1-Mediated Cell Death in *N. benthamiana* Requires the *At*EDS1 EP Domain

Next we tested whether the *At*EDS1 EP domain is necessary for XopQ-triggered cell death in *Nb-epss* (Figure 6). Because the EDS1 EP domain is unstable without its N-terminal lipase-like domain (Wagner et al., 2013), we compared activities of full-length *At*EDS1-FLAG and the FLAG-*At*EDS1 lipase-like domain (amino acids 1 to 384; Wagner et al., 2013), which accumulated to similar levels in *Nb-epss* leaves (Supplemental Figure 7A). The *At*EDS1 lipase-like domain did not confer XopQ-triggered cell death (Figures 6A), indicating a requirement for the *At*EDS1 EP domain in reconstituting *N. benthamiana* TNL (*Roq1*)-dependent cell death. We further tested effects of individually mutating two *At*EDS1 EP domain amino acids F419E and H476F, which are on the α-helical coil surface closest to the *At*SAG101 patch found to be necessary for Roq1-mediated cell death (Figure 6B). Mutations at the *Sl*EDS1 position F435, which corresponds to *At*EDS1 F419, impaired *Sl*EDS1 function in *Roq1*-dependent cell death (Gantner et al., 2019). Alongside the two *At*EDS1 mutants, we tested two *At*EDS1 variants that are nonfunctional in Arabidopsis TNL im-munity: *At*EDS1^{LLIF}, with very weak EDS1-partner N-terminal binding (Figures 1C and 6B; Wagner et al., 2013; Cui et al., 2018), and *At*EDS1^{R493A} with impaired EDS1-PAD4 heterodimer signaling (Bhandari et al., 2019). In the *Nb-epss* assays, *At*EDS1^{F419E} and *At*EDS1^{H476F} failed to confer *Roq1*-dependent cell death at 3 DAI, whereas *At*EDS1^{LLIF} and *At*EDS1^{R493A} were functional (Figure 6C). The YFP-tagged variants accumulated to similar or higher levels than wild-type *At*EDS1-YFP in *Nb-epss* leaves at 2 DAI (Supplemental Figure 7B). Combined with the *At*PAD4-*At*SAG101 chimera phenotypes (Figure 5), these data identify aligned parts of the *At*EDS1 and *At*SAG101 EP domains as being necessary for TNL-triggered cell death in *N. benthamiana*. Interestingly, the N-terminal LLIF contact and EP domain R493 that are required for *At*EDS1-*At*PAD4 basal and TNL immunity in

---

Figure 4. (continued).

YFP. The experiment was repeated three times independently (dots of the same color represent six technical replicates [leaf discs] from one independent experiment [biological replicate]). Statistical analysis was performed with a Nemenyi test ($\alpha = 0.01$, $n = 18$).

(C) Ion leakage assay in *Nb-epss* plants expressing *At*EDS1-FLAG in combinations with *At*PAD4-FLAG (P) or *At*SAG101-FLAG (S), *At*ADR1-L2-SH (A), and *At*NRG1.1-SH (N) and in the presence of XopQ-myc, as indicated. The measurement was performed at 3 DAI. "—" in sample descriptions refers to Agrobacteria-mediated YFP expression. *At*PAD4-FLAG and *At*ADR1-L2-SH cannot substitute *At*SAG101-FLAG or *At*NRG1.1-SH in the cell death re-constitution assay. The experiment was repeated three times independently (dots of the same color represent six technical replicates [leaf discs] from one independent experiment [biological replicate]). Statistical analysis was performed with a Nemenyi test ($\alpha = 0.01$, $n = 18$).

(D) *X. c. vesicatoria* growth assay in *Nb-epss* (gray) at 6 DAI after transiently expressing combinations of FLAG-*Sl*EDS1 (*Sl*), *At*EDS1-FLAG (*At*), *Nb*SAG101b-GFP (*Nb*-B), *At*SAG101-FLAG (*At*S), *At*PAD4-FLAG (*At*P), *At*ADR1-L2-SH (A), and *At*NRG1.1-SH (N). The experiment was repeated three times in-dependently (dots of the same color represent four technical replicates [extractions of bacteria] within one independent experiment [biological replicate]). Statistical analysis included a Tukey HSD test. Samples with different letter codes above bars indicate significant differences between means ($\alpha = 0.001$, $n = 12$). Error bars represent ±SEM. WT, wild type.

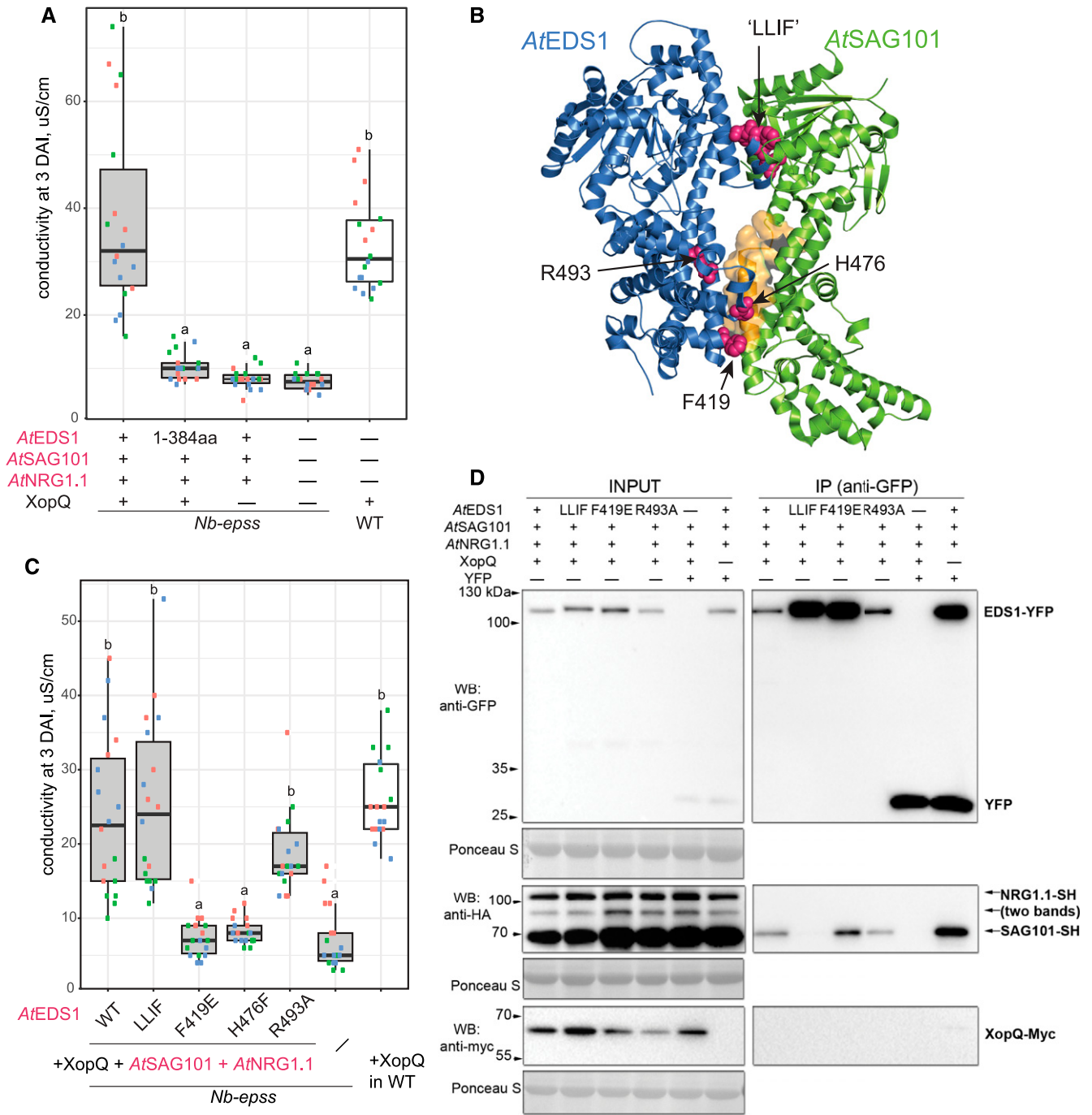**Figure 5.** Features in EP Domains of *At*SAG101 and *At*PAD4 Determine Difference in Their Functionality in Reconstituted TNL *Roq1*-Dependent Cell Death in *N. Benthamiana*.

(A) Schematic representation of *At*PAD4-*At*SAG101 chimeras used in assays shown in **(B)** and **(C)**. The *At*EDS1-*At*SAG101 crystal structure (PDB ID 4nfu) is used as background with *At*PAD4 or *At*SAG101 portions and amino acid positions shown in green or pink, respectively. *At*EDS1 is blue.

(B) Ion leakage assay quantifying XopQ-myc triggered cell death in *Nb-epss* plants (gray) expressing YFP-tagged *At*PAD4, *At*SAG101 or chimeras (chi1 to chi4, as indicated) with *At*EDS1-YFP, *At*NRG1.1-SH, and XopQ-myc. Cell death in wild type (WT; white) in response to XopQ served as a control. The experiment was performed three times (dots of the same color represent six technical replicates [leaf discs] from one independent experiment [biological replicate]). Statistical analysis was performed using a Nemenyi test. Samples with different letters above the box plots have statistically significant differences in conductivity ($\alpha = 0.01$, $n = 18$).

(C) Macroscopic cell death symptoms in the wild type (WT) and *Nb-epss* leaf panels at 3 days after agroinfiltration of the protein combinations shown in **(B)**. In contrast to the ion leakage assays, infiltrated leaves were wrapped in aluminum foil for 2 days and photographs taken at 3 DAI. Numbers under each image indicate necrotic/total infiltrated sites observed in three independent experiments. In **(B)** and **(C)**, "—" in the infiltration scheme refers to addition of *A. tumefaciens* strain to express YFP.

Figure 6. *At*EDS1 EP Domain Is Essential For Reconstituted *N. Benthamiana Roq1* Dependent Cell Death.

(A) Ion leakage assay quantifying cell death in the *N. benthamiana* wild type (WT; white) and *Nb-epss* (gray) after transient expression of XopQ-myc with *At*EDS1-FLAG (*At*EDS1), FLAG-*At*EDS1 lipase-like domain (*At*EDS1:1-384), *At*SAG101-YFP (*At*SAG101), *At*NRG1.1-SH (*At*NRG1.1), or YFP ("—" in the sample descriptions). The experiment was performed three times (dots of the same color represent six technical replicates [leaf discs] in each experiment [biological replicate]). Nemenyi test was applied to test for significance of differences in conductivity ($\alpha = 0.01$, $n = 18$).
(B) *At*EDS1 amino acids mutated in the structure-function analysis of *At*EDS1 activity in the reconstituted *Roq1*-dependent cell death. *At*EDS1 and *At*SAG101 are shown as blue and green ribbon diagrams, respectively. Ribbon and sphere depiction of the *At*EDS1-*At*SAG101 heterodimer crystal structure. Amino acids mutated in this analysis (LLIF, R493, H476, F419) are displayed as pink spheres. The portion of an *At*SAG101 EP domain central -helical coil identified as essential for cell death activity in *Nb-epss* reconstitution assays with chimeric *At*PAD4-*At*SAG101 proteins is represented as an orange surface.

Arabidopsis (Wagner et al., 2013; Cui et al., 2018; Bhandari et al., 2019) are dispensable for AtEDS1-AtSAG101 cooperation with AtNRG1.1 in the Nb-$epss$ TNL (Roq1)–mediated cell death response.

Transiently expressed NbNRG1-FLAG was found to interact by IP with NbEDS1a-HA in $N.$ $benthamiana$ (Qi et al., 2018). In addition, AtNRG1.1-FLAG association with AtEDS1-HA in $N.$ $benthamiana$ transient assays was reported when AtEDS1-HA was used as a bait (Wu et al., 2019). We tested for interaction between AtEDS1 and AtNRG1.1 using the functional AtEDS1-YFP–AtSAG101-SH–AtNRG1.1-SH module coexpressed with and without XopQ in Nb-$epss$ leaves (Figure 6D). Samples were collected at 2 d after agroinfiltration. In the presence of XopQ-myc, AtEDS1-YFP, AtEDS1^{F419E}-YFP and AtEDS1^{R493A}-YFP, but not AtEDS1^{LLIF}-YFP, interacted with AtSAG101-SH, consistent with their specific association driven by the AtEDS1 lipase-like domain (Wagner et al., 2013; Bhandari et al., 2019). We were unable to detect specific copurification of AtNRG1.1-SH with AtEDS1-YFP in these assays in the presence or absence of XopQ-myc.

EDS1 EP Domain Mutants Are Impaired in Arabidopsis $RRS1S$-$RPS4$ Cell Death

Analysis of the AtEDS1^{F419E} and AtEDS1^{H476F} mutants revealed the importance of these EP domain residues with AtSAG101 and AtNRG1.1 in $N.$ $benthamiana$ TNL cell death (Figure 6C). We examined whether immunity to $P.$ $s.$ $tomato$ $avrRps4$ in Arabidopsis Col mediated by TNL pair RRS1S-RPS4 was affected by these mutations. For this analysis, genomic AtEDS1^{F419E} and AtEDS1^{H476F} (gEDS1-YFP) constructs were transformed into Col $eds1$-2 and two independent homozygous transgenic lines expressing EDS1-YFP proteins (nos. 1 and 2) selected for each variant (Figure 7; steady state expression levels in Figure 7C). The lines were infiltrated with $P.$ $s.$ $tomato$ $avrRps4$ alongside the wild type Col, $eds1$-2 and functional gEDS1-YFP or signaling defective AtEDS1^{R493A} and AtEDS1^{LLIF} controls (Wagner et al., 2013; Cui et al., 2018; Bhandari et al., 2019). As expected, AtEDS1^{R493A} and AtEDS1^{LLIF} plants failed to restrict $P.$ $s.$ $tomato$ $avrRps4$ growth (Figure 7A). AtEDS1^{F419E} was also fully susceptible, but, surprisingly, AtEDS1^{H476F} retained $RRS1S$-$RPS4$ resistance (Figure 7B). We tested the same lines for TNL ($RRS1S$-$RPS4$) macroscopic cell death at 24 h after inoculation (HAI) after infiltration of $Pseudomonas$ $fluorescens$ 0-1 delivering AvrRps4 (Heidrich et al., 2011; Sohn et al., 2014). All variants (AtEDS1^{F419E}, AtEDS1^{H476F}, AtEDS1^{R493A}, and AtEDS1^{LLIF}) were defective in cell death (Figure 7B). Therefore, AtEDS1^{LLIF},

AtEDS1^{R493A}, and AtEDS1^{F419E} fail to limit bacterial growth and induce TNL ($RRS1S$-$RPS4$) cell death in Arabidopsis, whereas AtEDS1^{LLIF} and AtEDS1^{R493A}, but not AtEDS1^{F419E}, retain cell death–inducing activity in $N.$ $benthamiana$. More strikingly, AtEDS1^{H476F} was defective in cell death in Arabidopsis and $N.$ $benthamiana$ but fully competent in Arabidopsis TNL resistance to bacteria. These data suggest that the same AtEDS1 EP domain surface lining the AtEDS1-AtPAD4 or AtEDS1-AtSAG101 cavity controls bacterial TNL resistance and host cell death in Arabidopsis and $N.$ $benthamiana$ but that EDS1-SAG101 and EDS1-PAD4 EP domain signaling functions are different.

Different Genetic Requirements for Cell Death and Bacterial Growth Restriction in Arabidopsis RRS1/RPS4 Immunity

Evidence of AtEDS1-AtSAG101-AtNRG1 activity and AtEDS1-AtPAD4-AtNRG1 inactivity in $N.$ $benthamiana$ TNL-triggered cell death and resistance to bacteria (Figures 4 and 5) lends support to engagement of distinct AtSAG101/AtNRG1 and AtPAD4/AtADR1 immunity branches in Arabidopsis TNL signaling (Wu et al., 2019).

To test this, we quantified TNL ($RRS1S$-$RPS4$) bacterial resistance and cell death phenotypes in Arabidopsis Col $EDS1$-family single mutants ($eds1$-2, $pad4$-1, and $sag101$-3), a double mutant ($pad4$-1 $sag101$-3), and an AvrRps4 nonrecognizing mutant ($rrs1a$ $rrs1b$; Figure 8; Saucet et al., 2015). These mutant lines were tested alongside a CRISPR-associated 9 (Cas9)–generated Col AtNRG1.1 AtNRG1.2 double mutant line $nrg1.1$ $nrg1.2$ (denoted as $n2$; Supplemental Figure 8A; see Methods). Different Arabidopsis TNLs exhibited varying genetic dependencies on $NRG1$- and $ADR1$-family genes (Castel et al., 2018; Wu et al., 2019). In addition, NRG1 and ADR1 orthologs share phylogenetically distinct nucleotide binding domains (Supplemental Figure 8B; Collier et al., 2011; Shao et al., 2016). Therefore, we also generated a pentuple $nrg1.1$ $nrg1.2$ $adr1$ $adr1$-$L1$ $adr1$-$L2$ mutant (denoted as $n2a3$) by transforming the AtNRG1.1/AtNRG1.2 Cas9 mutagenesis construct into an $adr1$ $adr1$-$L1$ $adr1$-$L2$ triple mutant (denoted as $a3$; Supplemental Figure 8A; Bonardi et al., 2011).

At the level of $P.$ $s.$ $tomato$ $avrRps4$ growth at 3 DAI, the $sag101$ and $n2$ mutants exhibited wild-type Col resistance (Figure 8A). The $pad4$ and $a3$ mutants partially restricted bacterial growth, phenocopying $rrs1a$ $rrs1b$, whereas $eds1$, $pad4$ $sag101$, and $n2a3$ mutants were highly susceptible to $P.$ $s.$ $tomato$ $avrRps4$ (Figure 8A). These data show that AtADR1-family genes, like AtPAD4 (Feys et al., 2005; Wagner et al., 2013), genetically compensate for loss of AtSAG101 or AtNRG1 functions in $RRS1S$-

---

Figure 6. (continued).

(C) Ion leakage assay quantifying defects of AtEDS1-YFP mutants shown in **(B)** in Nb-$epss$ (gray) reconstituted Roq1-mediated cell death. Conductivity measured in Nb-$epss$ transiently expressing YFP ("−") and the $N.$ $benthamiana$ wild type (WT) expressing XopQ-myc (white) served as negative and positive controls, respectively. Experiments were performed three times independently (dots of the same color represent six technical replicates [leaf discs] from one independent experiment [biological replicate]). Samples with different letters above the box plots have statistically significant differences in conductivity after Nemenyi test ($\alpha = 0.01$, n=18).

(D) Co-IP assay to test interaction between AtEDS1 and AtNRG1.1 Nb-$epss$ after Agrobacteria-mediated transient expression of proteins. AtEDS1-YFP WT or indicated variants were coexpressed with AtSAG101-SH, AtNRG1.1-SH and XopQ-myc. YFP instead of AtEDS1-YFP was used as a negative control. Samples were collected 2 days after Agrobacteria infiltration. Experiments were performed three times independently with similar results.
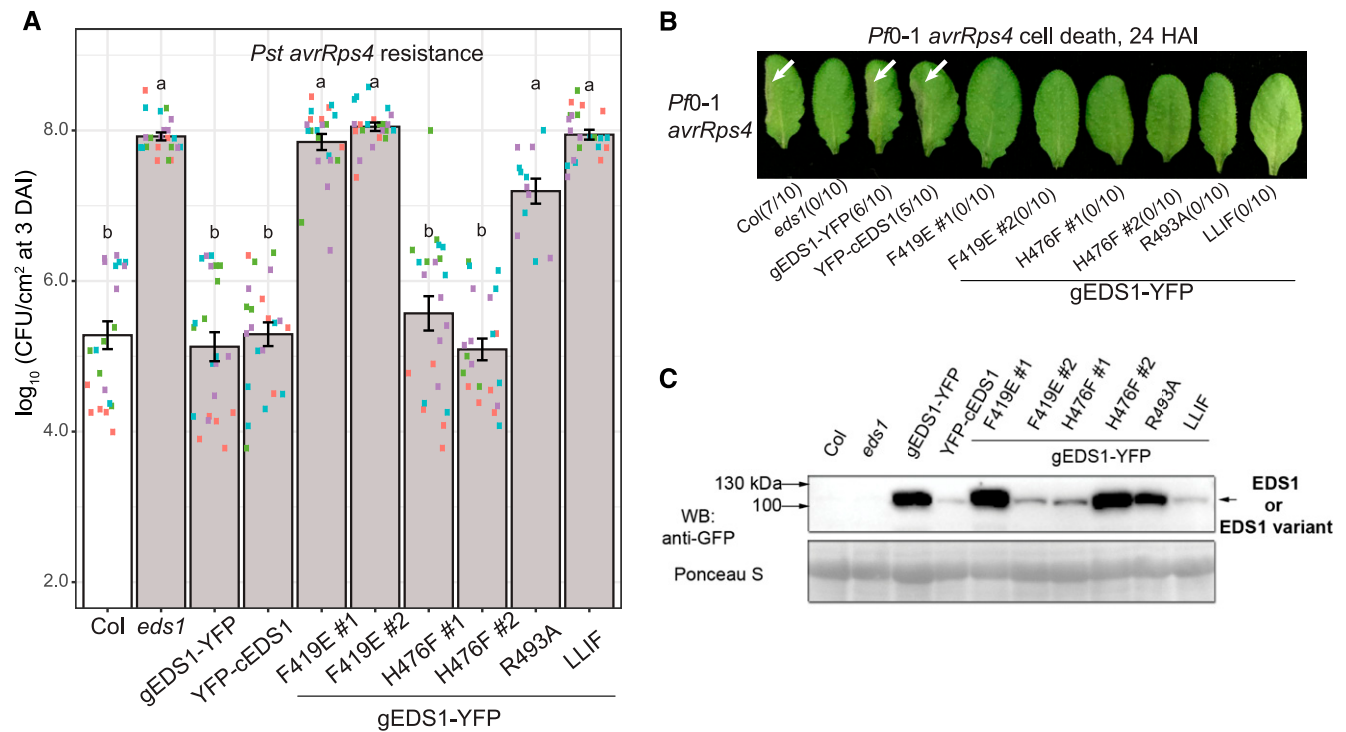
Figure 7. *At*EDS1 Variants With Mutated Lipase-Like and EP Domains Have Different Defects in Arabidopsis *RRS1S-RPS4*-Dependent Cell Death and Bacterial Growth Arrest.

(A) *P. s. tomato avrRps4* titers at 3 DAI (starting OD_{600} = 0.0005, syringe infiltration) in leaves of Arabidopsis Col *eds1-2* (gray) independent homozygous transgenic lines expressing Arabidopsis gEDS1-YFP and corresponding mutant variants (F419E, H476F, R493A, LLIF) under control of native pEDS1 promoter, as indicated. Responses in WT coding (cEDS1) and genomic (gEDS1) *At*EDS1 transgenic lines (gEDS1-YFP and YFP-cEDS1) and Col (white) served as controls. Experiments were performed four times (biological replicates; and twice for the R493A line), each with five technical replicates (extractions of bacteria). Statistical analysis used a Tukey HSD test and grouping of genotypes by letters at the significance threshold α = 0.001 (*n* = 10-20). CFU, colony forming units. Error bars represent ±SEM.

(B) Macroscopic cell death of Arabidopsis leaves of the same genotypes as used in **(A)**, visible as tissue collapse at 24 h after *P. fluorescens* 0-1 (*Pf* 0-1) *avrRps4* infiltration (OD_{600}=0.2). Experiments were repeated three times with similar results. Numbers in parentheses indicate leaves showing visual tissue collapse/infiltrated leaves in one representative experiment.

(C) Protein gel blot analysis of Arabidopsis lines expressing the YFP-tagged WT EDS1 and mutant variants tested in the **(A)** and **(B)**, before pathogen infiltration. The analysis was performed twice independently with similar results. Ponceau S staining of membrane shows equal protein loading.

RPS4 immunity and that combined loss of the *ADR1*- and *NRG1*-helper NLR family functions, like loss of *PAD4* and *SAG101* together, produce a fully defective TNL/EDS1 bacterial immune response.

We measured TNL (*RRS1S-RPS4*) cell death phenotypes in the same panel of mutants after infiltration with *P. fluorescens*0-1 *avrRps4* bacteria and monitoring ion leakage at 8 HAI (Figure 8B) and macroscopic cell death at 24 HAI (Figure 8C). Host cell death was strongly reduced in *eds1*, indicating it is *EDS1*-dependent (Heidrich et al., 2011; Sohn et al., 2014). The *pad4* and *a3* mutants exhibited a similar level of tissue collapse and ion leakage as the wild type Col-0 (Figures 8B and 8C) and therefore are dispensable for TNL (*RRS1S-RPS4*)–triggered cell death. The *sag101* and *n2* mutants phenocopied *rrs1a rrs1b* with an intermediate cell death response (Figures 8B and 8C). The *pad4 sag101* double and *n2a3* pentuple mutants phenocopied *eds1-2* (Figures 8B and 8C), indicating complete loss of *EDS1*-dependent host cell death when combined activities of *AtNRG1*- with *AtADR1*-family or *AtPAD4* with *AtSAG101* are lost. Compared with the *P. s. tomato avrRps4*

growth phenotypes (Figure 8A), these demarcations between cell death–competent and cell death–compromised lines (Figures 8B and 8C) point to a major role for *At*NRG1.1 and *At*NRG1.2 proteins with SAG101 in promoting TNL/EDS1-mediated cell death in Arabidopsis, which is dispensable for limiting bacterial growth when PAD4 and ADR1-family functions are intact. By contrast, EDS1/PAD4, likely together with ADR1-family proteins, have a major role in limiting bacterial growth in Arabidopsis TNL (*RRS1S-RPS4*) immunity but are dispensable for host cell death when SAG101 and NRG1 are active.

DISCUSSION

In dicotyledonous species, activated TNL receptors converge on the lipase-like protein EDS1, which transduces signals to downstream defense and cell death pathways to stop pathogen growth (Wiermer et al., 2005; García et al., 2010; Heidrich et al., 2011; Adlung et al., 2016; Qi et al., 2018; Gantner et al., 2019). In
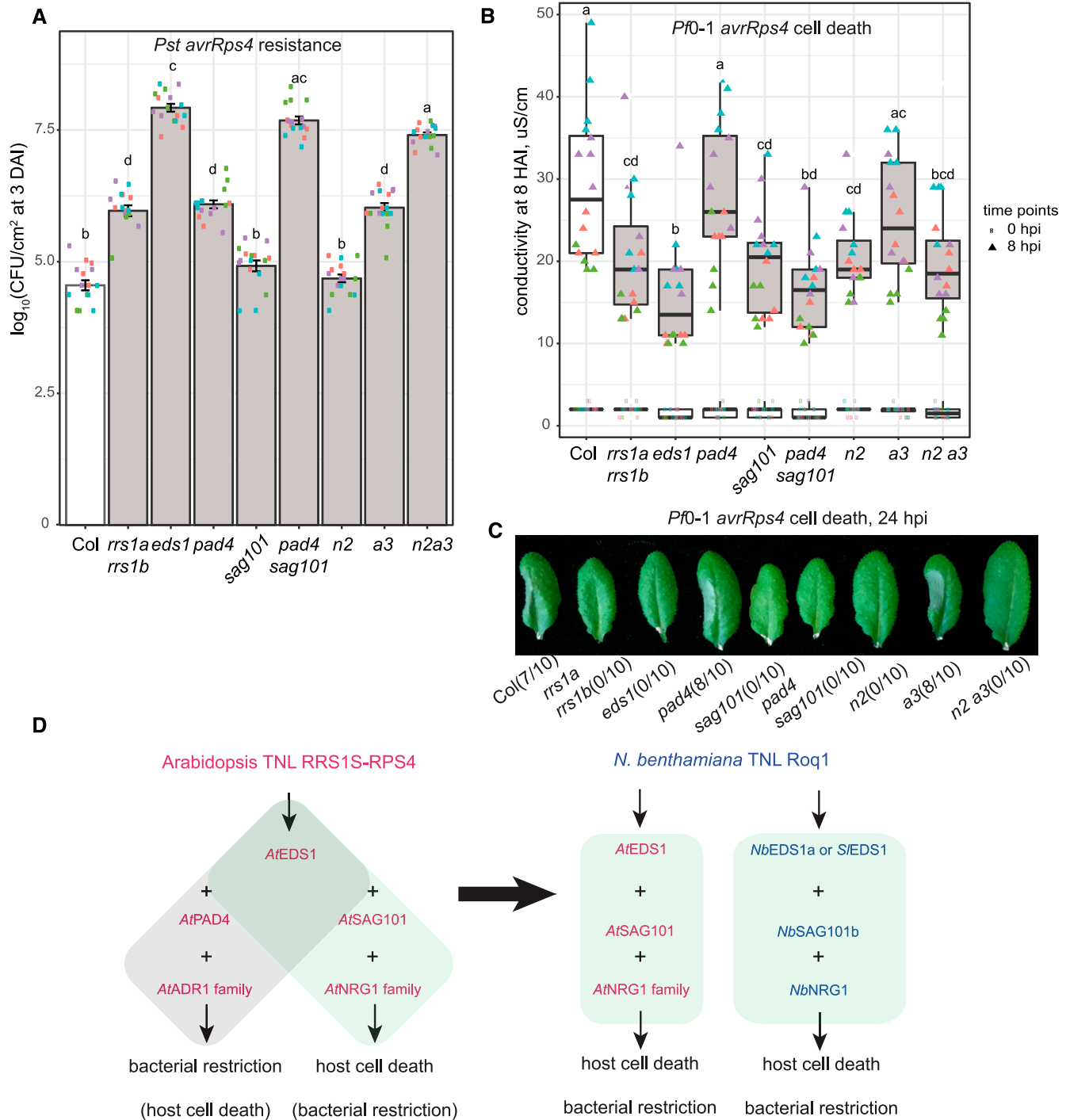
Figure 8. Differential Requirements for *EDS1*-, *NRG1*-, And *ADR1*-Family Genes in Arabidopsis RRS1S-RPS4-Mediated Cell Death and Bacterial Growth Arrest.

(A) *P. s. tomato avrRps4* titers at 3 DAI (OD_{600} = 0.0005) in leaves of Arabidopsis Col (white) and single or combinatorial mutants lines, as indicated. Experiments were performed four times independently (dots with the same colors represent technical replicates [extractions of bacteria] within the same experiment [biological replicate]). Letters above bars correspond to statistical grouping after a Tukey HSD test (α = 0.001, n = 16). Error bars represent ±SEM. **(B)** Ion leakage assay quantifying *P. fluorescens* 0-1 *avrRps4* (OD_{600}=0.2) cell death (at 8 HAI) in the Arabidopsis genotypes tested in **(A)**. The experiment was repeated four times independently (dots with the same color represent four technical replicates [four leaf discs] in one experiment [biological replicate]). Samples with overlapping letter codes above the whisker boxes do not show statistically significant differences (Tukey HSD, α = 0.001, n = 16).

Arabidopsis, *At*EDS1 functions in a heterodimer with one of its partners, *At*PAD4, to transcriptionally mobilize antimicrobial defense pathways and bolster SA-dependent programs that are important for basal and systemic immunity (Rietz et al., 2011; Wagner et al., 2013; Cui et al., 2017). *At*EDS1-*At*PAD4–mediated signaling is sufficient for basal immunity against virulent bacterial and oomycete pathogens and for ETI initiated by many TNL receptors (Wiermer et al., 2005). The function of *At*EDS1 heterodimers with its second partner, *At*SAG101, was not determined (Rietz et al., 2011; Xu et al., 2015). We show in this article that *At*EDS1 functions together with *At*SAG101 and *At*NRG1 helper CNL proteins as a coevolved host cell death signaling module in TNL ETI (Figures 4A, 4D, and 8A to 8C). We provide genetic and molecular evidence that *At*EDS1-*At*SAG101-*At*NRG1 promote TNL-dependent cell death in their native Arabidopsis (Figures 8B and 8C) and in a Solanaceous species, *N. benthamiana* (Figure 4A), with varying impacts on bacterial resistance. In both systems, the strong cell death activity cannot be substituted by *At*EDS1 with *At*PAD4 (Figures 4B to 4D and 5). We establish that *At*SAG101 and *At*NRG1.1/*At*NRG1.2 contribute to Arabidopsis TNL (*RRS1S-RPS4*)–dependent restriction of *P. s. tomato avrRps4* bacterial growth when *At*PAD4 and *At*ADR1-family genes are mutated (Figure 8A). In an *N. benthamiana* TNL (*Roq1*) reconstitution assay, the *At*EDS1-*At*SAG101-*At*NRG1.1 module confers cell death (Figures 4A to 4C) and limits *X. c. vesicatoria* bacterial growth (Figure 4D). Analysis of EDS1-family evolutionary rate variation (Supplemental Figure 1B) coupled with resistance/cell death phenotyping of targeted *At*EDS1 and *At*SAG101 protein variants provides additional evidence that EDS1-SAG101 has coevolved with NRG1 to promote TNL cell death and a structural basis (Figures 5 to –7) for understanding functionally distinct EDS1-SAG101 and EDS1-PAD4 branches in TNL-mediated immunity (Figure 8D).

A motivation for this study was to explore EDS1-family variation between different plant lineages to identify constraints that might influence protein functionality between distant clades. For this analysis, we first performed a large-scale phylogenetic analysis of EDS1-family orthologs across 46 seed plant species (Figure 1A; Supplemental Figure 1A; Supplemental Table 1; Supplemental Data Sets 1 to 3). This analysis identified well-supported phylogenetic groups for EDS1, PAD4, and SAG101 protein-coding sequences in Brassicaceae and Solanaceae and for EDS1 and PAD4 in Poaceae, Pinacea (conifers), and Caryophyllales, which lack *SAG101* genes (Supplemental Table 1). The analysis places the origins of the EDS1 family deep in the evolutionary history of

seed plants and not only angiosperms (Wagner et al., 2013). Although *EDS1* and *PAD4* are present in the majority of seed plants, *SAG101* has experienced dynamic evolution via loss in flowering plants (Supplemental Table 1). It is unclear whether *SAG101* emerged only in flowering species or existed earlier in a common ancestor of seed plants. Because *TNL* genes exist in seed plant species without *SAG101* and *NRG1*, as in conifers (Supplemental Table 1; Meyers et al., 2002) and in nonseed plants without an entire EDS1 family (Gao et al., 2018), it is possible that some TNLs signal without SAG101 and NRG1. Indeed, TNL Roq1 triggered effector XopQ-dependent cell death in *B. vulgaris* (Schultink et al., 2017), which does not have recognizable *SAG101* or *NRG1* genes (Supplemental Table 1).

Identification of conserved regions in EDS1, PAD4, and SAG101 (Supplemental Figure 1B) close to the EP domain interaction surfaces and at the LLIF α-helix (Supplemental Figure 1C) promoting EDS1-family heterodimerization (Wagner et al., 2013) suggested molecular possibilities for physical interactions between proteins from different taxonomic groups. A previous study of grape (*Vitis vinifera*) EDS1 forms expressed stably in Arabidopsis found a correlation between the ability of these proteins to interact with Arabidopsis PAD4 and resistance to powdery mildew infection (Gao et al., 2014). In this study, we extended the set of tested species beyond Rosids to Asterids and monocots. Examining EDS1 partner interactions within and between the angiosperm families Brassicaceae, Solanaceae, and Poaceae (Figure 1B; Supplemental Figure 2A) revealed conserved within-species or -clade partner associations but certain barriers to EDS1 heterodimer formation between groups. These data highlight EDS1-PAD4 heterodimer formation as necessary but not sufficient for Arabidopsis TNL-mediated immunity (Wagner et al., 2013; Gao et al., 2014; Bhandari et al., 2019).

Two recent studies of TNL and CNL receptor signaling in Arabidopsis show that TNL receptors utilize genetically redundant ADR1 (ADR1, ADR1-L1, and ADR1-L2) and NRG1 (NRG1.1, NRG1.2) helper NLR families to different extents for immunity (Castel et al., 2019; Wu et al., 2019). These and earlier reports (Bonardi et al., 2011; Dong et al., 2016) provide evidence that Arabidopsis ADR1 and NRG1 proteins work as parallel branches downstream of TNL activation. Genetic data supported *AtADR1*s and *AtPAD4* operating in the same *EDS1*-controlled pathway to bolster SA and other transcriptional defenses, whereas *AtNRG1*s were important for promoting host cell death (Bonardi et al., 2011; Dong et al., 2016; Castel et al., 2019; Wu et al., 2019). Several tested Arabidopsis TNLs recognizing oomycete pathogen strains,

---

Figure 8. (continued).

(C) Macroscopic cell death symptoms, visible as tissue collapse at 24 h after infiltration of *P. fluorescens*0-1 *avrRps4* (OD$_{600}$ = 0.2) into leaves of the Arabidopsis lines tested in **(A)**. Numbers in parentheses represent leaves showing tissue collapse/total infiltrated leaves in one experiment. One experiment is shown as representative of three independent experiments.

(D) Schematic showing cooperation between EDS1-family proteins and ADR1 or NRG1 helper NLRs in Arabidopsis and *N. benthamiana* TNL immune responses tested in this study. In Arabidopsis, RRS1S-RPS4 recognition of AvrRps4 in ETI bolsters EDS1-PAD4-ADR1 immune responses leading to restriction of *P. s. tomato avrRps4*. A different RRS1S-RPS4 ETI pathway mediated by EDS1-SAG101-NRG1 promotes host cell death but these components are dispensable for limiting bacterial growth if the EDS1-PAD4-ADR1 branch is operational. A complete Arabidopsis TNL immune response requires cooperation between the two branches. In *N. benthamiana*, TNL Roq1-conditioned bacterial (*X. c. vesicatoria*) growth arrest and cell death are channeled through the EDS1-SAG101-NRG1 signaling module and thus do not require EDS1-PAD4. Cross-clade transfer of a compatible Arabidopsis EDS1-SAG101-NRG1 module is sufficient to signal Roq1-mediated cell death and resistance to *X. c. vesicatoria* infection.

a TNL autoimmune allele of Suppressor of Npr1-1, Constitutive1 (SNC1), and TNL pair CHS3/CSA1 displayed varying dependence on *AtNRG1* signaling in immunity (Castel et al., 2019; Wu et al., 2019). By contrast, all TNL pathogen resistance and cell death responses tested so far in *N. benthamiana* signaled via *NbEDS1a*, *NbNRG1*, and *NbSAG101b* but did not require *NbPAD4* (Adlung et al., 2016; Qi et al., 2018; Gantner et al., 2019). Similarly, we found a dependency of TNL *Roq1* resistance and cell death responses to *X. c. vesicatoria* bacteria on *NbEDS1a* and *NbSAG101b* but not *NbPAD4* (Figure 3). Collectively, these data suggest that whereas there is TNL signaling choice in Arabidopsis, a strong pathway preference exists in *N. benthamiana* for *EDS1* with *SAG101* and *NRG1*.

Further support for a TNL-branched resistance signaling model (Figure 8D) comes from quantifying Arabidopsis TNL (*RRS1S-RPS4*) *P. s. tomato avrRps4* growth and *P. fluorescens* 0-1 *avrRps4* cell death phenotypes in *ADR1*-family triple (*a3*; Bonardi et al., 2011), double (*n2*), and combined (pentuple; *n2a3*) mutants, alongside *EDS1*-family mutants (Figures 8A to 8C). Importantly, effects of *pad4* and *sag101* single mutations on Arabidopsis *RRS1S-RPS4* resistance and cell death responses were, respectively, phenocopied by the *a3* and *n2* mutants (Figures 8A to 8C). Proposed PAD4-ADR1 and SAG101-NRG1 cofunctions in bacterial immunity (Figure 8D) are in line with Arabidopsis *NRG1*-like genes regulating *SAG101*-dependent *chs3-2d* autoimmunity (Xu et al., 2015; Wu et al., 2019) and *ADR1*-like genes regulating *PAD4*-dependent *snc1* autoimmunity (Zhang et al., 2003; Dong et al., 2016). This proposal is also supported by a strong signature of joint loss of SAG101 and NRG1 orthologs in several groups of flowering plants (Figure 1; Supplemental Table 1) and of EDS1, PAD4, and ADR1 orthologs in aquatic angiosperms (Baggs et al., 2019).

The Arabidopsis TNL (*RRS1S-RPS4*) phenotypic outputs measured in this study indicate that each branch contributes to a complete *EDS1*-dependent immune response (Figures 8A and 8B), pointing to potential synergistic activities and thus a degree of crosstalk between the two immunity arms, as proposed for Arabidopsis *snc1* autoimmunity (Wu et al., 2019). Our data suggest that a clean distinction between *AtEDS1/AtNRG1/AtSAG101*-controlled host cell death and *AtEDS1/AtADR1/AtPAD4*-mediated transcriptional promotion of defenses is not justified because *AtPAD4* and *AtADR1*s account for a small but measurable portion of *RRS1S-RPS4/EDS1*–dependent cell death in the Arabidopsis *sag101* and *n2* mutant backgrounds (Figure 8B). Reciprocally, *AtSAG101* and *AtNRG1* provide some *RRS1S-RPS4/EDS1* resistance to bacterial growth in the *pad4* and *adr1* mutants (Figures 8A to 8C). These features point to some compensation between the two branches in Arabidopsis that might aid TNL resilience against disabling of one or other immunity function. *AtSAG101* and *AtNRG1* contributions to Arabidopsis transcriptional reprogramming are not known, but in *N. benthamiana*, TNL (*Roq1*) and *EDS1*-dependent cell death and bacterial resistance were abolished by mutations in *SAG101b* (Figure 3; Gantner et al., 2019) and *NRG1* (Qi et al., 2018). Interestingly, *Roq1*-dependent transcriptional reprogramming was almost entirely dependent on *EDS1a* and largely dependent on *NRG1* (Qi et al., 2018), suggesting that other minor *EDS1*-dependent pathways are at play in TNL Roq1 immunity. Because Roq1 mediates XopQ-triggered cell

death in *B. vulgaris* (Schultink et al., 2017), which does not have recognizable SAG101 or NRG1 orthologs (Supplemental Table 1), this TNL might also have a capacity to function via a non-SAG101/NRG1 branch. It will be of interest to test whether PAD4 and ADR1 or other components are responsible for a set of transcriptional outputs in *N. benthamiana* TNL responses.

It is significant that *SlEDS1*, although not contributing with *SlPAD4* or *NbPAD4* to TNL (*Roq1*) mediated *X. c. vesicatoria* resistance or cell death in *N. benthamiana* (Figure 3; Gantner et al., 2019), is functional in TNL (*RPP4 and RRS1S-RPS4*) dependent resistance, when transferred stably to Arabidopsis (Figures 2B and 2C). Thus, *SlEDS1-SlPAD4* has an immunity activity, which we presume is required for some pathogen encounters in Solanaceae hosts. Because *AtEDS1-AtPAD4* heterodimers utilize the same EP domain surface (involving R493) for bacterial resistance conferred by a TNL (RRS1S-RPS4) and a CNL receptor RPS2 (Bhandari et al., 2019), it is possible that maintenance of *EDS1* and *PAD4* genes across seed plants (Supplemental Table 1) also reflects recruitment by certain CNLs, which can be masked by compensatory defense pathways (Venugopal et al., 2009; Tsuda et al., 2013; Cui et al., 2017; Mine et al., 2018). In contrast to *SlEDS1-SlPAD4* transferable function to Arabidopsis TNL-mediated immunity (Figures 2B and 2C), the *AtEDS1-AtSAG101* heterodimer was not active in *N. benthamiana* TNL (*Roq1*)-dependent cell death unless coexpressed with *AtNRG1.1* or *AtNRG1.2* (Figure 4A). In addition, interaction between *SlEDS1* and *AtSAG101* (Supplemental Figure 2A) was insufficient for *Roq1* signaling with otherwise functional *AtNRG1.1* or *NbNRG1* proteins (Figures 3D to 3F, 4B, and 4D). These data further highlight the existence of between-clade barriers to immunity function beyond *AtEDS1-AtSAG101* and *AtEDS1-AtPAD4* heterodimer formation (Figures 1B and 1C; Supplemental Figure 2A). The requirement for matching Arabidopsis proteins to constitute a functional EDS1-SAG101-NRG1 cell death module points to coevolutionary constraints existing not only on variable NLR receptor complexes (Concepcion et al., 2018; Schultink et al., 2019) but also on immunity signaling components.

The EDS1 structure-guided analyses presented here (Figures 5 to 7) and in Gantner et al. (2019) show that a conserved EDS1 EP domain–signaling surface is necessary for TNL cell death in Arabidopsis and *N. benthamiana*. The same EP domain surface is required for rapid mobilization of transcriptional defenses and restriction of bacterial growth in Arabidopsis *RRS1S-RPS4* ETI (Bhandari et al., 2019). Unexpectedly, two *At*EDS1 variants, *At*EDS1[LLIF] and *At*EDS1[R493A], that are defective in Arabidopsis *RRS1S-RPS4*–dependent bacterial resistance and cell death (Figure 7), are functional in the *N. benthamiana Roq1*–dependent cell death reconstitution assay (Figure 6D). This difference might be due to a requirement in Arabidopsis for *At*EDS1[LLIF] and *At*EDS1[R493A] (with *At*PAD4) to transcriptionally regulate their own expression and expression of important immunity components (Cui et al., 2018; Bhandari et al., 2019). That transcriptional role is dispensed with in the *N. benthamiana Roq1* assay because *At*EDS1, *At*SAG101, and *At*NRG1 proteins are transiently overexpressed. It will be interesting to examine whether failure of *At*PAD4 and/or *At*ADR1 to signal in *N. benthamiana* TNL *Roq1*-dependent resistance or cell death (Figures 4B to 4D) is because of the transient assay used or mismatches with other *N. benthamiana*

immunity components. These data reinforce functional distinctions between *At*PAD4 and *At*SAG101 in TNL/EDS1 signaling, as indicated by the *At*PAD4–*At*SAG101 chimeras that locate a specific portion of the *At*SAG101 EP domain conferring cell death in *N. benthamiana Roq1*–dependent responses (Figure 5).

With identification of an EP domain surface at the EDS1-SAG101 heterodimer cavity that is important for TNL dependent cell death (Figures 5 to 7; Gantner et al., 2019), it is tempting to speculate that the Arabidopsis EDS1-SAG101 heterodimer forms a complex with *At*NRG1.1 or *At*NRG1.2 to transmit TNL receptor activation to cell death pathways. We assessed whether this model is supported by our data. First, mutation of the *At*EDS1 LLIF α-helix, which strongly reduces *At*EDS1-*At*SAG101 dimerization (Wagner et al., 2013; Cui et al., 2018), did not disable *Roq1*-reconstituted cell death in *Nb-epss* plants (Figure 6D). We cannot rule out that partial impairment of EDS1^LLIF^-SAG101 heterodimerization is compensated for by protein overexpression in the *N. benthamiana* assay. Second, subcellular localizations of transiently expressed *At*SAG101 and *At*NRG1 proteins tested in our *N. benthamiana* experiments show that *At*SAG101 is mainly nuclear (Supplemental Figure 2B), as observed in Arabidopsis on transient expression (Feys et al., 2005). By contrast, N- and C-terminally GFP-tagged *At*NRG1.1 and *At*NRG1.2 isoforms are mainly cytoplasmic (Supplemental Figure 5C). A cytoplasmic endomembrane accumulation pattern was also detected in Arabidopsis stable transgenic lines and *N. benthamiana* transient assays for functional *At*NRG1-mNeonGreen isoforms, which did not obviously change on TNL activation (Wu et al., 2019). Third, we did not detect specific interactions in IP between transiently expressed *At*EDS1 and *At*NRG1.1 with and without *At*EDS1-bound *At*SAG101 or coexpressed XopQ (Figure 6D), which is similar to the findings in Wu et al. (2019))). These data are difficult to reconcile with direct interaction between *At*EDS1 or *At*EDS1-*At*SAG101 and *At*NRG1 underlying cofunction in *N. benthamiana* (Figures 4A and 4B), although a small overlapping pool of these proteins might confer cell death activity. In this regard, it is notable that a cytoplasmic AvrRps4 pool elicited *EDS1*-dependent cell death in Arabidopsis *RRS1-RPS4* immunity (Heidrich et al., 2011). Moreover, *N. benthamiana Nb*NRG1 was reported to interact with *Nb*EDS1a in *N. benthamiana* (Qi et al., 2018), implying a molecular link between these immunity signaling components. It will be important in the future to resolve the modes and sites of action of NLR cell death and resistance signaling modules.

METHODS

Plant Materials and Plant Growth Conditions

Arabidopsis (*Arabidopsis thaliana*) Col mutants *eds1-2*, *pad4-1*, *sag101-3*, *pad4-1 sag101-3*, *eds1-2 pad4-1 sag101-1* were described previously by Glazebrook et al. (1997), Feys et al. (2005), Bartsch et al. (2006), Wagner et al. (2013), and Cui et al. (2018). The mutant *eds1-2 pad4-1 sag101-3* was selected from a segregating F2 population *eds1-2 pad4-1* x *sag101-3* (Cui et al., 2018). The Col *adr1 adr1-L1 adr1-L2* triple mutant was kindly provided by J. Dangl (Bonardi et al., 2011). *Nicotiana benthamiana* mutants *eds1a*, *eds1a pad4*, *pad4 sag101a sag101b* were described previously by Ordon et al. (2017) and Gantner et al. (2019). The quadruple *N. benthamiana eds1a pad4 sag101a sag101b* mutant was selected from a cross between *eds1a* and *pad4 sag101a sag101b*

mutants (Gantner et al., 2019). Genotyping was performed with Phire polymerase (F124; Thermo Fisher Scientific) on DNA extracted with the Suc or Edwards method (Berendzen et al., 2005). Oligonucleotides for genotyping are provided in Supplemental Table 3. Arabidopsis homozygous transgenic Col *eds1-2* lines expressing Col coding and genomic *At*EDS1 sequence (pEN *pAtEDS1:YFP-cAtEDS1*, pXCG *pAtEDS1:gAtEDS1-YFP*, *pAtEDS1:gAtEDS1^LLIF^-YFP*, *pAtEDS1: gAtEDS1^R493A^-YFP*) were described previously by García et al. (2010), Wagner et al. (2013), Cui et al. (2018), and Bhandari et al. (2019). Arabidopsis plants for bacterial infiltration assays were grown for 4 to 5 weeks under a 10-h-light (80–150 μMol/m²·s)/14-h-dark regimen at 22°C/20°C and ~65% relative humidity. Arabidopsis plants were kept under the same conditions after infiltration. Before assays, *N. benthamiana* plants were grown for 5 to 6 weeks under a 16-h-light/8-h-dark regimen at ~24°C.

Vector Generation by Gateway Cloning

Coding sequences of *EDS1* and *PAD4* with stop codons were amplified from cDNA potato (*Solanum tuberosum*; DM 1-3), barley (*Hordeum vulgare* cv Golden Promise), and *Brachypodium distachyon* (BD21-3). Arabidopsis Col genomic and coding *EDS1*, *PAD4*, and *SAG101* sequences were cloned previously (Feys et al., 2005; García et al., 2010; Wagner et al., 2013). Sequences of *AtNRG1.1* (AT5G66900.1), extended *AtNRG1.1* (AT5G66900.2), and *AtNRG1.2* (AT5G66910) were PCR-amplified using genomic DNA of Col as a template from start to stop codons. PCR amplification for all cloning was performed with Phusion (F530; Thermo Fisher Scientific) or PrimeStar HS (R010A; Clontech) polymerases. All sequences were cloned into pENTR/ D-TOPO (K240020; Thermo Fisher Scientific) and verified by Sanger sequencing. Sequences of oligonucleotides used for cloning are provided in Supplemental Table 3. Entry clones for *Sl*EDS1 and *Sl*PAD4 from cv VF36 were described previously by Gantner et al. (2019). *AtNRG1.1* and *AtNRG1.2* sequences without stop codons were obtained by site-directed mutagenesis of the pENTR/D-TOPO constructs with stop codons. Recombination into pB7GWF2.0 (Karimi et al., 2002), pB7FWG2.0 (Karimi et al., 2002), pDEST_GAD424 (Mitsuda et al., 2010), pDEST_BTM116 (Mitsuda et al., 2010), pAM-PAT-GW-3xFLAG, pXCSG-GW-3xFLAG, pXCSG-GW-StrepII-3xHA, pXCG-GW-StrepII-3xHA (Witte et al., 2004), pXCSG-GW-mYFP (with *At*NRG1.1_Stop and *At*NRG1.2_Stop to generate nontagged expression constructs; Witte et al., 2004), pXCG-GW-3xFLAG, pXCG-GW-mYFP, and pENSG-YFP (Witte et al., 2004) as well as custom pENpAtPAD4 StrepII-YFP (Supplemental Data Set 5 with sequence in .gbk format) was performed using LR Clonase II (11791100; Life Technologies).

Vector Generation by Golden Gate Cloning

Level 0 constructs for coding sequences of *Sl*EDS1, *Sl*PAD4, *At*EDS1, *At*PAD4, *Nb*SAG101b, and promoter sequences of *At*EDS1 and *At*PAD4 were described previously (Gantner et al., 2018, 2019). *Hv*EDS1 and *Hv*PAD4 from cultivar Golden Promise were cloned into level 0 pICH41308. Synthesized (GeneArt; ThermoFisher Scientific) coding sequence of *Nb*SAG101a was cloned into the level 0 vector pAGM1287. At level 1, Arabidopsis, tomato (*Solanum lycopersicum*), and barley *PAD4* coding sequences were cloned into pICH47811 (*pAtPA-D4:YFP-xxPAD4-35S_term*) and *EDS1* into pICH47802 (*pAtEDS1:3x-FLAG-xxEDS1-35S_term*). For level 2 constructs in pAGM4673, the *PAD4* expression module was placed at position 1, *EDS1* at position 2, and *pNos:BASTA^R^-Nos_term* (pICSL70005) cassette at position 3. The *35S:NbSAG101a-GFP-35S_term* and *35S:NbSAG101b-GFP-35S_term* expression constructs were cloned into pICH47802.

Backbones (pAGM1287, pICH41308, pICH47802, pICH47811), tags (pICSL30005, pICSL30004, pICSL50008), and 0.4 kb CaMV35S promoter (pICH51277) and terminator (pICH41414) modules as well as the BASTA^R expression cassette (pICSL70005) are from the Golden Gate cloning toolkit (Engler et al., 2014). Sequences of oligonucleotides used for cloning are provided in Supplemental Table 3.

Site-Directed Mutagenesis and Generation of AtPAD4-AtSAG101 Chimeras

To substitute stop codons for Ala in pENTR/D-TOPO AtNRG1.1, pENTR/D-TOPO AtNRG1.2 and to introduce F419E and H476F mutations in pENTR/D-TOPO pAtEDS1:gAtEDS1 (García et al., 2010), the QuikChange II Site-Directed mutagenesis protocol (no. 200555; Agilent) was used with hot start polymerases Phusion (F530; ThermoFisher Scientific) or Prime Star (R010A; Takara). The pDONR207 AtPAD4-AtSAG101 chimeric sequences were generated by overlapping PCR with oligonucleotides in Supplemental Table 3 and LR recombined into pENSG-mYFP (Witte et al., 2004) or a modified pENSG-mYFP with a CaMV 35S promoter substituted for a 1083 bp AtPAD4 region upstream of start codon (Supplemental Data Set 5 with sequence "pENpAtPAD4 StrepII-mYFP-GW.gbk"). In the expression constructs, AtPAD4-AtSAG101 chimeras were N-terminal tagged: 35S:mYFP-chimera for cell death reconstitution assays or pAtPAD4:StrepII-mYFP-chimera for localization assays.

Y2H Assays

`Coding sequences of Arabidopsis (At), tomato (Sl), potato (St), barley (Hv) and B. distachyon EDS1 and PAD4 in pENTR/D-TOPO were LR-recombined into gateway-compatible pDEST_GAD424 (Gal4 Activation Domain [AD]) and pDEST_BTM116 (LexA BD; Mitsuda et al., 2010), respectively. The yeast (Saccharomyces cerevisiae) Leu, Trp, His (LWH) auxotroph strain L40 was used. No 3-amino-1,2,4-triazole (3-AT) was added to SDS selection plates without LWH. Yeast growth on selection plates LW and without LWH was recorded at 3 d after transformation.

Transient Expression (Agroinfiltration) Assays in N. benthamiana

N. benthamiana plants for agroinfiltration assays were grown under long-day conditions (24°C) for 5 to 6 weeks. Expression constructs (pAGM4673 pAtEDS1:3xFLAG-xxEDS1/pAtPAD4:YFP-xxPAD4 [xx stands for donor species At, Sl or Hv], pICH47811 pAtPAD4:YFP-AtPAD4, pICH47802 pAtEDS1:3xFLAG-SlEDS1, pICH47802 35S:NbSAG101a-GFP, pICH47802 35S:NbSAG101b-GFP, pXCG pAtEDS1:gAtEDS1-YFP wild type or LLIF, R493A, H476F, F419E variants, pXCG pAtEDS1:gAtEDS1-3xFLAG, pXCG pAtEDS1:gAtEDS1^{LLIF}-3xFLAG, pENS 35S:3xFLAG-cAtEDS1$^{1-384}$, 35S:AtNRG1.1_stop and 35S:AtNRG1.2_stop without a tag in pXCSG-mYFP, pXCSG 35S:AtNRG1.1-SH, pXCSG 35S:AtNRG1.2-SH, pB7WGF2.0 35S:GFP-AtNRG1.1, pB7WGF2.0 35S:GFP-AtNRG1.2, pB7GWF2.0 35S:AtNRG1.1-GFP, pB7GWF2.0 35S:AtNRG1.2-GFP, pXCSG 35S:gAtSAG101-SH, pXCSG 35S:gAtSAG101-YFP, pXCSG 35S:gAtSAG101-3xFLAG, pXCG pADR1-L2:ADR1-L2-SH, pAM-PAT 35S:cPAD4-3xFLAG, pICH47811 pAtPAD4:YFP-AtPAD4, pXCSG 35S:AtPAD4-YFP, pENSG 35S:SH-AtPAD4, pENSG 35S:mYFP-AtPAD4/AtSAG101 chimeras 1–4, pENS pAtPAD4:StrepII-mYFP-AtPAD4/AtSAG101 chimeras 1–4, pAM-PAT 35S:YFP) were electroporated into Rhizobium radiobacter (Agrobacterium tumefaciens) GV3101 pMP90RK or pMP90. Final OD$_{600}$ for each strain was set to 0.2, each sample contained A. tumefaciens C58C1 pCH32 to express 35S:p19 (final OD$_{600}$ = 0.2). Before syringe infiltration, A. tumefaciens was incubated in induction buffer (10 mM MES pH 5.6, 10 mM MgCl$_2$, 150 nM acetosyringone) for 1 to 2 h in the dark at room temperature.

Immunoblot Analysis

To test accumulation of proteins in N. benthamiana transient expression assays, four 8-mm leaf discs each were harvested at 2 DAI, ground in liquid nitrogen to powder, and boiled in 150 µL 2× Laemmli buffer for 10 min at 95°C. For Arabidopsis lines, four 8-mm leaf discs or four to five seedlings per sample were processed in the same manner. The proteins were resolved on 8% (v/v) or 10% (v/v) SDS-PAGE (1610156, Bio-Rad) and transferred using the wet transfer method onto a nitrocellulose membrane (10600001, GE Healthcare Life Sciences). For protein detection, primary antibodies (anti-GFP [no. 2956, Cell Signaling Technology, or no. 11814460001, Roche], anti-HA [no. 3724, Cell Signaling Technology, or no. 11867423001, Roche], anti-FLAG [F7425 or F1804, Sigma-Aldrich], anti-myc [no. 2278, Cell Signaling Technologies]) were used in the dilution 1:5000 (1× TBST, 3% [v/v] milk powder, 0.01% [v/v] NaAz). Secondary HRP-conjugated antibodies (A9044 and A6154, Sigma-Aldrich; sc-2006 and sc-2005, Santa Cruz) were applied in the dilution 1:5000. Detection of the signal was performed with enhanced luminescence assays Clarity and Clarity Max (1705061 and 1705062, Bio-Rad) or SuperSignal West Pico and Femto (34080 and 34095, Thermo Fisher Scientific) using ChemiDoc (Bio-Rad). For loading control, membranes were stained with Ponceau S (09276-6X1EA-F, Sigma-Aldrich).

Immunoprecipitation Assays

Five 10-mm leaf discs were collected from N. benthamiana leaves at 2 to 3 d after agroinfitration and ground in liquid nitrogen. All further steps were performed at 4°C if not mentioned otherwise. Soluble fraction was extracted in 5 mL of the buffer containing 50 mM Tris-HCl, pH 7.5, 150 mM NaCl, 10% (w/w) glycerol, 5 mM DTT, 1% (w/w) Triton X-100, and EDTA-free 1× Plant Protease Inhibitor Cocktail (11873580001, Sigma-Aldrich). Debris was removed by 2× 15-min centrifugation at 14,000g. IPs were performed with 10 µL of anti-FLAG M2 Affiinity Gel slurry (A2220, Sigma-Aldrich) or GFP-trapA beads (gta-100, Chromotek). After 2.5 h of incubation under constant rotation, beads were washed in 4 to 5 mL of the extraction buffer and eluted by boiling in 100 µL of 2× Laemmli for 10 min at 95°C.

Xanthomonas Infection Assays in the Presence of A. tumefaciens

Xanthomonas campestris pv vesicatoria (85-10; also Xanthomonas euvesicatoria; Thieme et al., 2005), kindly provided by Ulla Bonas, was added to A. tumefaciens mixes to a final OD$_{600}$ = 0.0005. A. tumefaciens strains were prepared as for the transient expression assays without a P19 expressing strain with the exception of assays shown in Figure 4D, where the P19-expressing strain was included. To ensure equal OD$_{600}$ in all samples, A. tumefaciens expressing p35S:YFP was used in all experiments as filler. The bacterial mix was syringe-infiltrated into N. benthamiana leaves. A. tumefaciens pAtEDS1:3xFLAG-SlEDS1 complemented X. c. vesicatoria susceptibility in N. benthamiana eds1a in an OD$_{600}$ range of 0.05 to 0.6. For consistency between the cell death assays, a final A. tumefaciens OD$_{600}$ = 0.2 was used for each strain. After infiltration, plants were placed in a long-day chamber (16 h light/8 h dark at 25°C/23°C). Bacteria were isolated at 0 DAI (three 8-mm leaf discs served as three technical replicates) and 6 DAI (four 8-mm leaf discs representing four technical replicates), and dilutions were dropped onto medium made of peptone, yeast extract, glycerol, and agar (NYGA) supplemented with rifampicin 100 mg/L and streptomycin 150 to 200 mg/L. In statistical analysis of X. c. vesicatoria titers at 6 DAI, results from independent experiments (biological replicates) were combined. Normality of residuals distribution and homogeneity of variance was assessed visually and by Shapiro–Wilcoxon and Levene tests (P > 0.05). If both conditions were met, ANOVA was followed by

Tukey honestly significant difference (HSD) test ($\alpha = 0.001$), otherwise the Nemenyi test with Bonferroni correction for multiple testing was applied ($\alpha = 0.01$).

Cell Death Assays in *N. benthamiana*

After agroinfiltration, *N. benthamiana* plants were placed under a 16-h-light/8-h-dark regimen at 22°C. Six 8-mm leaf discs from *N. benthamiana* agroinfiltrated leaves were taken at 3 DAI, washed in 10 to 20 mL of milliQ water (18.2 MΩ*cm, mQ) for 30 to 60 min, transferred to a 24-well plate with 1 mL mQ in each well, and incubated at room temperature. Ion leakage was measured at 0 and 6 h with a conductometer Horiba Twin Model B-173. For statistical analysis, results of measurements at 6 h for individual leaf discs (each leaf disc represents a technical replicate) were combined from independent experiments (biological replicates). Data were checked for normality of residuals distribution and homogeneity of variance using visual examination of the plots and Shapiro–Wilcoxon and Levene tests ($P > 0.05$). If both conditions were met, ANOVA was followed by the Tukey HSD post hoc test ($\alpha = 0.001$). Otherwise, a nonparametric Nemenyi test with Bonferroni correction for multiple testing was applied ($\alpha = 0.01$). For visual assessment of cell death symptoms, infiltrated leaves were covered in aluminum foil for 2 d and opened to "dry" the lesions and enhance visual symptoms at 3 DAI.

Pseudomonas Infection and Cell Death Assays in Arabidopsis

Pseudomonas syringae pv *tomato* DC3000 *pVSP61 avrRps4* (Hinsch and Staskawicz, 1996) was syringe-infiltrated into leaves at $OD_{600} = 0.0005$ in 10 mM $MgCl_2$. After infiltration, lids were kept on trays for 24 h and then removed. Bacteria were isolated at 0 DAI (six to eight 5-mm leaf discs making three or four technical replicates) and 3 DAI (ten to twelve 5-mm leaf discs distributed over five or six technical replicates). Dilutions were plated onto NYGA plates supplemented with rifampicin 100 mg/L and kanamycin 25 mg/L. For statistical analysis, bacterial titers from independent experiments (biological replicates) were combined. Normality of residuals distribution and homoscedasticity was checked visually and with formal Shapiro–Wilcoxon and Levene tests ($\alpha = 0.05$). Collected titer data were considered suitable for ANOVA and the Tukey HSD test ($\alpha = 0.001$). For cell death assays, *Pseudomonas fluorescens* 0-1 *pEDV6 avrRps4* (Sohn et al., 2014) was grown at 28°C on King's B medium (tetracycline 5 mg/l, chloramphenicol 30 mg/l), resuspended at a final $OD_{600} = 0.2$ in 10 mM $MgCl_2$, and syringe-infiltrated into leaves. Ten leaves (technical replicates) per genotype were infiltrated for each independent experiment (biological replicate). Ion leakage assays were performed at 0 and 8 HAI as described (Heidrich et al., 2011), with an independent experiment considered as a biological replicate. Cell death symptoms visible as collapse of infiltrated areas of leaves were recorded at 24 HAI.

Hyaloperonospora arabidopsidis Ewma1 Infection Assays

Seedlings from segregating (3:1) Arabidopsis T3 transgenic lines coexpressing 3× FLAG-EDS1 and YFP-PAD4 from Arabidopsis or tomato were preselected at 10 d on one half Murashige and Skoog plates supplemented with phosphinothricin (PPT, 10 mg/l). A Col *35S:StrepII-3xHA-YFP* transgenic line and *eds1-2 pad4-1 sag101-1* used as controls were pregrown on PPT plates alongside the test lines. Ws-2 seedlings were grown on one half Murashige and Skoog plates without PPT. After selection, seedlings were transplanted onto soil in Jiffy pots and grown for an additional 7 d under a 10-h-light/14-h-dark, 22°C/20°C regimen. *H. arabidopsidis* Emwa1 spray inoculation (40 conidiospores per microliter of distilled water) was performed as described (Stuttmann et al., 2011). *H. arabidopsidis*

colonization was quantified by counting conidiospores on leaves at 7 DAI. In statistical analysis, counts normalized per milligram of fresh weight (five counts used as technical replicates) from independent experiments (biological replicates) were combined. Significance of difference in spore counts was assessed with a nonparametric Nemenyi test and Bonferroni correction for multiple testing ($\alpha = 0.01$).

Laser Scanning Fluorescence Microscopy

Analysis of protein subcellular localization after transient expression in *N. benthamiana* was performed 2 to 3 DAI with the exception *At*NRG1.1 and *At*NRG1.2 experiments performed at 1 DAI to avoid quenching of GFP signal due to *At*NRG1.2-triggered cell death. Fluorescence signals in 8-mm leaf discs transiently expressed proteins were recorded on a laser-scanning confocal microscope (LSM780 or LSM700; Zeiss) and generally under conditions when intensity of only a small fraction of pixels was saturated. Z-stacks were projected with ZEN (Zeiss) or Fiji using maximum intensity or sD methods. Used objectives were 40× (numerical aperture [NA]: 1.3 oil or 1.2 water) and 63× (NA: 1.4 oil or 1.2 water).

Generation of Arabidopsis *n2* and *n2a3* Mutants

Arabidopsis *n2* and *n2a3* mutants were generated using targeted mutagenesis with the CRISPR (clustered regularly interspaced short palindromic repeats)–Cas9 method. Six guide RNAs (Supplemental Table 3) were designed to target the first two exons in *AtNRG1.1* and *AtNRG1.2* using CRISPR-P 2.0 (Liu et al., 2017). *AtNRG1.3* was not targeted because it is likely a pseudogene (Castel et al., 2019; Wu et al., 2019). Two arrays of three fusions, the *pU6:sgRNA_backbone-Pol_III_terminator*, each were synthesized (GeneArt; Thermo Fisher Scientific) based on a template (Peterson et al., 2016) with flanking SbfI/PmeI/SmaI sites for merging via restriction–ligation. The merged single array was further cloned into the pKIR1.0 (Tsutsui and Higashiyama, 2017) at the SbfI restriction site. To generate *n2* and *n2a3* mutant lines, the construct was electroporated into *A. tumefaciens* GV3101 pMP90RK for subsequent floral dip transformation (Logemann et al., 2006) into Col and Col *adr1 adr1-L1 adr1-L2* (Bonardi et al., 2011), respectively. T1 plants with active gRNA-Cas9 were preselected with the T7 endonuclease 1 assay (Hyun et al., 2015) or by direct sequencing of PCR products covering the target regions. Absence of the *Cas9* construct in lines homozygous for the *nrg1.1 nrg1.2* double mutation in *n2* and *n2a3* was tested with PCR using oligonucleotides matching the *Hyg* resistance gene in the T-DNA insertion and visually as lack of red fluorescence in the seed coat (Tsutsui and Higashiyama, 2017). One homozygous line free of the mutagenesis construct was selected for *n2* and *n2a3*. Mutations detected in the *AtNRG1.1* and *AtNRG1.2* genes in *n2* and *n2a3* lines are shown in Supplemental Figure 8A. Oligonucleotides used for genotyping of the mutants are listed in Supplemental Table 3.

Identification of Orthogroups

To build orthogroups (OGs) from predicted 52 plant proteomes (listed in Supplemental Table 4), results of bidirectional BLASTP search (all versus all, E-value cutoff 1^{e-3}, ncbi-blast-2.2.29+; Altschul et al., 1990) were used for orthology inference in orthomcl (version 2.0.9, E-value cutoff is 1^{e-5}) with the mcl clustering tool (version 14-137; Li et al., 2003). This resulted in 99,696 OGs. OrthoMCL-generated OGs for EDS1, PAD4, and SAG101 were further verified with BLASTP (e-value: 0.00001) against Arabidopsis (The Arabidopsis Information Resource 10). The original SAG101 OG appeared to be contaminated with AT3G01380, whereas EDS1 and PAD4 OGs contained only respective Arabidopsis hits. To systematically filter for high-confidence EDS1-family orthologs, EDS1, PAD4, and BLASTP-verified SAG101 sequences were tested for the presence of EP domain

(Hidden-Markov Model [HMM] profile for EP domain in Supplemental Data Set 6, hmmsearch–incE 0.00001 in HMMER 3.1b2 [Eddy, 2011], ≥50 amino acid–long match). EP domain HMM was obtained with hmmbuild (in HMMER 3.1b2 [Eddy, 2011], default parameters) using MUSCLE multiple sequence alignment for EP domain sequences found by BLASTP (e-value: 0.01) with EP domains of *At*EDS1 (Q9XF23 385-623), *At*PAD4 (Q9S745 300-541), *At*SAG101 (Q4F883 291-537) (Wagner et al., 2013) against proteomes of 32 plant species from algae to Arabidopsis (Supplemental Table 5). Finally, sequences that were too short (≤400 amino acids) and too long (≥1200) in OrthoMCL-derived OGs were removed. A full pipeline and scripts to extract EP sequences and build HMMs are in the GitHub repository "Lapin_Kovacova_Sun_et_al." Filtered EDS1-family OGs are referred to as "high confidence orthologs" (Supplemental Data Sets 1– to 3). Their counts are given in Supplemental Table 1. BLASTP against The Arabidopsis Information Resource 10 did not detect contamination of ADR1 and NRG1 OrthoMCL OGs with other proteins. Their counts are also provided in Supplemental Table 1.

Additional manual searches for EDS1-family and NRG1 orthologs were performed using reciprocal BLASTP with Arabidopsis EDS1, PAD4, SAG101 and NRG1.1 sequences against spinach (*Spinacia oleracea*, bvseq.molgen.mpg.de; v.1.0.1), raspberry (*Rubus occidentalis*, v1.0.a1; VanBuren et al., 2016), jujube (*Ziziphus jujube*; Liu et al., 2014), sesame (*Sesamum indicum*, Sinbase; v1.0), and quinoa (*Chenopodium quinoa*; Zou et al., 2017). *Nb*EDS1-family sequences were obtained with tblasn searches of tomato sequences EDS1-family sequences on solgenomics.net and match sequences (Ordon et al., 2017; Gantner et al., 2019). To search for EDS1, PAD4, ADR1, and NRG1 orthologs in *Silene* genus (Balounova et al., 2019), BLASTX (-word_size 4 -evalue 1[e-20]) was performed with Arabidopsis amino acid sequences against nonfiltered de novo transcriptome assemblies. We considered a gene to be present in the assembly if the Arabidopsis sequence had a significant match with a unique contig.

Phylogenetic and Conservation Analyses

Full-length EDS1-family sequences including high-confidence EDS1, PAD4, and SAG101 orthologs (Supplemental Data Sets 1 to 3) and additional sequences from literature and other databases are provided in Supplemental Data Set 4. To prepare EDS1-family ML tree, the EDS1-family protein sequence alignment produced with mafft (version mafft-7.221, linsi, 100 iterations; Katoh et al., 2002; Katoh and Standley, 2013) was filtered using Gblocks (gap positions <50%; number of contiguous nonconserved positions: 15; minimum length of conserved block: 4; Castresana, 2000; Talavera and Castresana, 2007), leaving 101 positions in 12 blocks (Supplemental Data Sets 7 and 8). The best evolutionary model (JTT+G) was selected with protTest3 (Darriba et al., 2011) based on the Bayesian information criterion. The best ML tree was calculated with RAxML v.8.1.21 (rapid bootstrap analysis and search for a best-scoring maximum-likelihood tree in one run -f a, 1000 bootstraps; Stamatakis, 2014). For Bayesian inference of EDS1-family protein phylogeny, we used MrBayes 3.2.6 with the same alignment as used for the ML tree (5 million generations, four runs; amino acid model: mixture of models, gamma rates; Huelsenbeck and Ronquist, 2001; Ronquist and Huelsenbeck, 2003). Annotated phylogenetic trees were midpoint rooted and are available via iTOL (for a link, see Accession Numbers; Letunic and Bork, 2016).

For the best nucleotide binding domain found in Apaf-1, R proteins, and the CED-4 (NBARC) domain ML tree, NBARC domain sequences were extracted based on the tabular output of hmmsearch (–incE 0.01, HMMER 3.1b2 [Eddy, 2011]; PFAM PF00931.21 pfam.xfam.org) and aligned with mafft (version mafft-7.407, linsi, 1000 maximum iterations; Katoh et al., 2002; Katoh and Standley, 2013). The NBARC domain alignment without editing was supplied to RAxML (v.8.2.10, -f a, 800 bootstraps, LG model

with empirical amino acid frequencies proposed via -m PROTGAM-MAAUTO; this model was also selected as best fitting in protTest3 [Darriba et al., 2011]). Gblocks-filtered NBARC domain alignment produced similar topology but lower bootstrap support values on almost all branches. The annotated NBARC phylogenetic tree is available via iTOL (for a link, see Accession Numbers; Letunic and Bork, 2016).

For calculations of EDS1-family evolutionary conservation rates, amino acid sequences were aligned with mafft (version mafft-7.221-without-extensions, linsi, 100 iterations). Branch lengths of ML phylogenetic trees for EDS1, PAD4, and SAG101 built with RAxML (version standard-RaxML-8.1.21; Stamatakis, 2014) were optimized with the rate4site package (version rate4site-3.0.0, default parameters, background optimization with gamma model; Pupko et al., 2002). Mapping of the evolutionary rates onto the structure *At*EDS1-*At*SAG101 or homology-based model *At*EDS1-*At*PAD4 (Wagner et al., 2013) was performed in PyMol v2.0.7.

Positive Selection Tests for *EDS1*

Analyses of evolutionary pressure acting on the *EDS1* sequence as a whole and per site were performed with the Phylogenetic Analysis by Maximum Likelihood (PAML) package (Yang, 2007). The CODEML program of PAML 4.9a (Yang, 2007) was used to estimate the ratio (ω) of the nonsynonymous substitution rate to the synonymous substitution rate. In all models, the reference tree was an unrooted ML phylogenetic tree of EDS1 sequences with optimized branch lengths (CODEML program with the codon model M0 and the site model NS0, as recommended in the PAML FAQ document [page 14, http://abacus.gene.ucl.ac.uk/software/pamlFAQs.pdf]). The equilibrium frequencies of codons were calculated from the nucleotide frequencies (CodonFreq = 2) using jmodeltest-2.1.10 (Guindon et al., 2003; Darriba et al., 2012). All models listed in Supplemental Table 2 were modeled with the following initial ω-values: 0.1, 0.5, 1, and 2. Because multinucleotide mutations can lead to false inference of positive selection (Venkat et al., 2018), we provide alignments at positions with inferred positive selection in *Brassicaceae* EDS1 (Supplemental Figure 1D).

R Packages Frequently Used in This Study

The following R packages were utilized (R core team 2016, bio-conductor.org): ggplot2 (http://ggplot2.org; 3.0.0), PMCMRplus (https://CRAN.R-project.org/package=PMCMRplus; 1.0.0), multcompView (https://CRAN.R-project.org/package=multcompView; 0.1-7), bioStrings (2.42.1).

Accession Numbers

Accession numbers of EDS1, PAD4 and SAG101 orthologs used in the study: *At*EDS1 (AT3G48090.1), *At*PAD4 (AT3G52430.1), *At*SAG101 (AT5G14930.2), *Sl*EDS1 (Solyc06g071280.2.1), *Sl*PAD4 (Solyc02g032850.2.1), *St*EDS1 (PGSC0003DMP400055762), *St*PAD4 (PGSC0003DMP400034509), *Bd*EDS1 (XP_003578076.1), *Bd*PAD4 (XP_003577748.1), *Hv*EDS1 (MLOC_67615.1), *Hv*PAD4 (HORVU4Hr1G043530.1), *Nb*SAG101a (Niben101Scf00271g02011.1), *Nb*SAG101b (Niben101Scf01300g01009.1).

Accession numbers of NBARC-containing proteins used to infer phylogenetic placement of ADR1 and NRG1 NBARC domains: *At*NRG1.1 (Q9FKZ1), *At*NRG1.2 (Q9FKZ0), *Nb*NRG1 (Q4TVR0), *Sl*ADR1 (Solyc04g079420), *Os*ADR1 (LOC_Os12g39620.3), *Hv*ADR1 (A0A287QlD5), *At*ADR1 (Q9FW44), *At*ADR1-L1 (Q9SZA7), *At*ADR1-L2 (Q9LZ25), *Sl*Bs4 (Q6T3R3), *Lus*L6 (Q40253), *Nb*Roq1 (A0A290U7), *At*RPP1 (F4J339), *At*RPP4 (F4JNA9), *At*RPS4 (Q9XGM3), *At*RPS2 (Q42484), *Os*RLS1 (Q6Z6E7), *St*Rx (Q9XGF5), AT5G56220 (Q9FH17), *Cc*Bs2 (Q9SNW0), *Sl*NRC1 (A1X877), *Sl*NRC2 (K4CZZ5), *Hv*MLA10 (Q6WWJ4), *At*RPP8 (Q8W4J9), *At*RPM1 (Q39214), *At*ZAR1 (Q38834).

Annotated EDS1-family phylogenetic trees (ML and Bayesian) and ML tree for NBARC domains from selected NLR proteins: https://itol.embl.de/shared/lapin.

Content of GitHub repository "Lapin_Kovacova_Sun_et_al": pipeline and scripts to derive EP domain HMM (subdirectory "EP_domain_HMM"), pipeline and scripts used to filter OrthoMCL EDS1-family OG and obtain high-confidence sequences (subdirectory "high_confidence_OG"), R-code for statistical analysis.

Supplemental Data

Supplemental Figure 1. Phylogenetic and conservation analysis of EDS1-family protein sequences.

Supplemental Figure 2. Arabidopsis EDS1 does not interact with *Nb*SAG101a and *Nb*SAG101b in *N. benthamiana.*

Supplemental Figure 3. Complementation of *Roq1*-dependent resistance to *X. c. vesicatoria* and cell death signaling in *Nb-epss* using agrobacteria-mediated transient expression.

Supplemental Figure 4. Initial characterization of N- and C-terminally eGFP- or SH-tagged *At*NRG1.1 or *At*NRG1.2 after transient expression in *N. benthamiana* under the control of the 35S promoter.

Supplemental Figure 5. Protein accumulation in assays to test *At*SAG101 EP domain activity in the Roq1 cell death reconstitution assays in *Nb-epss*.

Supplemental Figure 6. Subcellular localization of *At*PAD4/*At*-SAG101 chimeric proteins in *Nb-epss*.

Supplemental Figure 7. Protein accumulation in assays to find sequence and structural determinants of *At*EDS1 activity in *Nb-epss* Roq1 cell death reconstitution.

Supplemental Figure 8. Mutants for NRG1-family genes generated in this study and phylogenetic relationships between main NLR groups inferred based on NB-ARC domains.

Supplemental Table 1. Counts of EDS1, PAD4, SAG101, ADR1, and NRG1 orthologs in 52 green plants.

Supplemental Table 2. Selection pressure acting on *EDS1* sequences in poaceae, solanaceae, and brassicaceae.

Supplemental Table 3. Sequences of oligonucleotides used in this study.

Supplemental Table 4. Names of 52 green plant species used in the OrthoMCL analysis.

Supplemental Table 5. Names of 32 green plant species used to build EP domain hidden-markov model (HMM) profile.

Supplemental Data Set 1. Sequences of high-confidence EDS1 orthologs (fasta format).

Supplemental Data Set 2. Sequences of high-confidence PAD4 orthologs (fasta format).

Supplemental Data Set 3. Sequences of high-confidence SAG101 orthologs (fasta format).

Supplemental Data Set 4. Sequences of EDS1-family proteins used for ML and bayesian phylogeny inference (fasta format).

Supplemental Data Set 5. Sequence of the custom destination gateway vector pENpAtPAD4 strepII-YFP (.gbk format).

Supplemental Data Set 6. EP domain hidden-markov model (HMM) profile.

Supplemental Data Set 7. Gblocks-filtered alignment of EDS1-family sequences used for the phylogenetic analysis with RAxML and MrBayes.

Supplemental Data Set 8. Correspondence between EDS1-family sequence names on the phylogenetic trees and in public databases.

AUTHOR CONTRIBUTIONS

J.E.P. and D.L. conceived the project. D.L. designed, coordinated, and performed experiments; generated the *n2 a3* mutant; and prepared the GitHub repository with input from V.K. V.K. designed and performed orthology inference and phylogenetic analyses. X.S., N.G., D.B., P.v.B, J.B., J.A.D., and J.R. performed experiments. J.A.D. designed CRISPR-Cas9 mutagenesis constructs and generated the *n2* mutant. D.B. designed and generated structure-guided mutants. J.B. selected the *Nb-epss* mutant and did EDS1/PAD4 ortholog cloning. J.S. provided *Nb-pss* mutants, an F2-segregating population to select *Nb-epss* and modules for Golden Gate cloning, and pENTR/D-TOPO clones of tomato EDS1 and PAD4. A.B. contributed to orthology analysis and discussions. D.L. and J.E.P. wrote the article with input from all coauthors.

REFERENCES

Adlung, N., Prochaska, H., Thieme, S., Banik, A., Blüher, D., John, P., Nagel, O., Schulze, S., Gantner, J., Delker, C., Stuttmann, J., and Bonas, U. (2016). Non-host resistance induced by the *Xanthomonas* effector XopQ is widespread within the genus *Nicotiana* and functionally depends on EDS1. Front. Plant Sci. **7:** 1796.

Altschul, S.F., Gish, W., Miller, W., Myers, E.W., and Lipman, D.J. (1990). Basic local alignment search tool. J. Mol. Biol. **215:** 403–410.

Ariga, H., et al. (2017). NLR locus-mediated trade-off between abiotic and biotic stress adaptation in Arabidopsis. Nat. Plants **3:** 17072.

Asai, S., Furzer, O.J., Cevik, V., Kim, D.S., Ishaque, N., Goritschnig, S., Staskawicz, B.J., Shirasu, K., and Jones, J.D.G. (2018). A downy mildew effector evades recognition by polymorphism of expression and subcellular localization. Nat. Commun. **9:** 5192.

Baggs, E., Dagdas, G., and and Krasileva, K.V. (2017). NLR diversity, helpers and integrated domains: Making sense of the NLR IDentity. Curr. Opin. Plant Biol. **38:** 59–67.

Baggs, E.L., Thanki, A.S., O'Grady, R., Schudoma, C., Haerty, W., and Krasileva, K.V. (2019). Convergent gene loss in aquatic plants predicts new components of plant immunity and drought response.

bioRxiv: Cold Spring Harbor Laboratory. https://www.biorxiv.org/content/10.1101/572560v1https://doi.org/10.1101/572560.

Balounova, V., et al. (2019). Evolution of sex determination and heterogamety changes in section Otites of the genus Silene. Sci. Rep. **9:** 1045.

Bartsch, M., Gobbato, E., Bednarek, P., Debey, S., Schultze, J.L., Bautor, J., and Parker, J.E. (2006). Salicylic acid–independent ENHANCED DISEASE SUSCEPTIBILITY1 signaling in Arabidopsis immunity and cell death is regulated by the monooxygenase FMO1 and the Nudix hydrolase NUDT7. Plant Cell **18:** 1038–1051.

Berendzen, K., Searle, I., Ravenscroft, D., Koncz, C., Batschauer, A., Coupland, G., Somssich, I.E., and Ülker, B. (2005). A rapid and versatile combined DNA/RNA extraction protocol and its application to the analysis of a novel DNA marker set polymorphic between Arabidopsis thaliana ecotypes Col-0 and Landsberg erecta. Plant Methods **1:** 4.

Bhandari, D.D., Lapin, D., Kracher, B., von Born, P., Bautor, J., Niefind, K., and Parker, J.E. (2019). An EDS1 heterodimer signalling surface enforces timely reprogramming of immunity genes in Arabidopsis. Nat. Commun. **10:** 772.

Bhattacharjee, S., Halane, M.K., Kim, S.H., and Gassmann, W. (2011). Pathogen effectors target Arabidopsis EDS1 and alter its interactions with immune regulators. Science **334:** 1405–1408.

Bonardi, V., Tang, S., Stallmann, A., Roberts, M., Cherkis, K., and Dangl, J.L. (2011). Expanded functions for a family of plant intracellular immune receptors beyond specific recognition of pathogen effectors. Proc. Nat. Acad. Sci. **108:** 16463–16468.

Castel, B., Ngou, P.M., Cevik, V., Redkar, A., Kim, D.S., Yang, Y., Ding, P., and Jones, J.D.G. (2019). Diverse NLR immune receptors activate defence via the RPW8-NLR NRG1. New Phytol. **222:** 966–980.

Castresana, J. (2000). Selection of conserved blocks from multiple alignments for their use in phylogenetic analysis. Mol. Biol. Evol. **17:** 540–552.

Collier, S.M., Hamel, L.-P., and Moffett, P. (2011). Cell death mediated by the N-terminal domains of a unique and highly conserved class of NB-LRR protein. Mol. Plant Microbe Interact. **24:** 918–931.

Concepcion, J.C.D.l., Franceschetti, M., Maqbool, A., Saitoh, H., Terauchi, R., Kamoun, S., and Banfield, M.J. (2018). Polymorphic residues in rice NLRs expand binding and response to effectors of the blast pathogen. Nat. Plants **4:** 576–585.

Cui, H., Tsuda, K., and Parker, J.E. (2015). Effector-triggered immunity: From pathogen perception to robust defense. Annu. Rev. Plant Biol. **66:** 487–511.

Cui, H., Gobbato, E., Kracher, B., Qiu, J., Bautor, J., and Parker, J.E. (2017). A core function of EDS1 with PAD4 is to protect the salicylic acid defense sector in Arabidopsis immunity. New Phytol. **213:** 1802–1817.

Cui, H., Qiu, J., Zhou, Y., Bhandari, D.D., Zhao, C., Bautor, J., and Parker, J.E. (2018). Antagonism of transcription factor MYC2 by EDS1/PAD4 complexes bolsters salicylic acid defense in Arabidopsis effector-triggered immunity. Mol. Plant **11:** 1053–1066.

Darriba, D., Taboada, G.L., Doallo, R., and Posada, D. (2011). ProtTest 3: Fast selection of best-fit models of protein evolution. Bioinformatics **27:** 1164–1165.

Darriba, D., Taboada, G.L., Doallo, R., and Posada, D. (2012). jModelTest 2: More models, new heuristics and parallel computing. Nat. Methods **9:** 772.

Dong, O.X., Tong, M., Bonardi, V., Kasmi, F.E., Woloshen, V., Wünsch, L.K., Dangl, J.L., and Li, X. (2016). TNL-mediated immunity in Arabidopsis requires complex regulation of the redundant ADR1 gene family. New Phytol. **210:** 960–973.

Eddy, S.R. (2011). Accelerated profile HMM searches. PLOS Comput. Biol. **7:** e1002195.

Engler, C., Youles, M., Gruetzner, R., Ehnert, T.-M., Werner, S., Jones, J.D.G., Patron, N.J., and Marillonnet, S. (2014). A Golden Gate modular cloning toolbox for plants. ACS Synth Biol. **3:** 839–843.

Feys, B.J., Moisan, L.J., Newman, M.A., and Parker, J.E. (2001). Direct interaction between the Arabidopsis disease resistance signaling proteins, EDS1 and PAD4. EMBO J. **20:** 5400–5411.

Feys, B.J., Wiermer, M., Bhat, R.A., Moisan, L.J., Medina-Escobar, N., Neu, C., Cabral, A., and Parker, J.E. (2005). Arabidopsis SENESCENCE-ASSOCIATED GENE101 stabilizes and signals within an ENHANCED DISEASE SUSCEPTIBILITY1 complex in plant innate immunity. Plant Cell **17:** 2601–2613.

Gantner, J., Ordon, J., Ilse, T., Kretschmer, C., Gruetzner, R., Löfke, C., Dagdas, Y., Bürstenbinder, K., Marillonnet, S., and Stuttmann, J. (2018). Peripheral infrastructure vectors and an extended set of plant parts for the Modular Cloning system. PLoS One **13:** e0197185.

Gantner, J., Ordon, J., Kretschmer, C., Guerois, R., and Stuttmann, J. (2019). An EDS1–SAG101 complex functions in TNL-mediated immunity in Solanaceae. bioRxiv: Cold Spring Harbor Laboratory. https://www.biorxiv.org/content/10.1101/511956v2 .

Gao, F., Dai, R., Pike, S.M., Qiu, W., and Gassmann, W. (2014). Functions of EDS1-like and PAD4 genes in grapevine defenses against powdery mildew. Plant Mol. Biol. **86:** 381–393.

Gao, Y., Wang, W., Zhang, T., Gong, Z., Zhao, H., and Han, G.-Z. (2018). Out of water: The origin and early diversification of plant R-genes. Plant Physiol. **177:** 82–89.

García, A.V., Blanvillain-Baufumé, S., Huibers, R.P., Wiermer, M., Li, G., Gobbato, E., Rietz, S., and Parker, J.E. (2010). Balanced nuclear and cytoplasmic activities of EDS1 are required for a complete plant innate immune response. PLoS Pathog. **6:** e1000970.

Glazebrook, J., Zook, M., Mert, F., Kagan, I., Rogers, E.E., Crute, I.R., Holub, E.B., Hammerschmidt, R., and Ausubel, F.M. (1997). Phytoalexin-deficient mutants of Arabidopsis reveal that *PAD4* encodes a regulatory factor and that four *PAD* genes contribute to downy mildew resistance. Genetics **146:** 381–392.

Guindon, S., Gascuel, O., and Rannala, B. (2003). A simple, fast, and accurate algorithm to estimate large phylogenies by maximum likelihood. Syst. Biol. **52:** 696–704.

Heidrich, K., Wirthmueller, L., Tasset, C., Pouzet, C., Deslandes, L., and Parker, J.E. (2011). Arabidopsis EDS1 connects pathogen effector recognition to cell compartment–specific immune responses. Science **334:** 1401–1404.

Hinsch, M., and Staskawicz, B. (1996). Identification of a new Arabidopsis disease resistance locus, RPS4, and cloning of the corresponding avirulence gene, avrRps4, from *Pseudomonas syringae* pv. *pisi*. Mol. Plant Microbe Interact. **9:** 55–61.

Holub, E.B. (1994). Phenotypic and genotypic characterization of interactions between isolates of *Peronospora parasitica* and accessions of *Arabidopsis thaliana*. Mol. Plant Microbe Interact. **7:** 223.

Huelsenbeck, J.P., and Ronquist, F. (2001). MRBAYES: Bayesian inference of phylogenetic trees. Bioinformatics **17:** 754–755.

Hyun, Y., Kim, J., Cho, S.W., Choi, Y., Kim, J.-S., and Coupland, G. (2015). Site-directed mutagenesis in *Arabidopsis thaliana* using dividing tissue-targeted RGEN of the CRISPR/Cas system to generate heritable null alleles. Planta **241:** 271–284.

Jones, J.D.G., Vance, R.E., and Dangl, J.L. (2016). Intracellular innate immune surveillance devices in plants and animals. Science **354:** aaf6395.

Jubic, L.M., Saile, S., Furzer, O.J., Kasmi, F.E., and Dangl, J.L. (2019). Help wanted: Helper NLRs and plant immune responses. Curr. Opin. Plant Biol. **50:** 82–94.

Karimi, M., Inzé, D., and Depicker, A. (2002). GATEWAY vectors for Agrobacterium-mediated plant transformation. Trends Plant Sci. **7:** 193–195.

Katoh, K., and Standley, D.M. (2013). MAFFT multiple sequence alignment software version 7: Improvements in performance and usability. Mol. Biol. Evol. **30:** 772–780.

Katoh, K., Misawa, K., Kuma, K.I., and Miyata, T. (2002). MAFFT: A novel method for rapid multiple sequence alignment based on fast Fourier transform. Nucleic Acids Res. **30:** 3059–3066.

Kim, T.-H., Kunz, H.-H., Bhattacharjee, S., Hauser, F., Park, J., Engineer, C., Liu, A., Ha, T., Parker, J.E., Gassmann, W., and Schroeder, J.I. (2012). Natural variation in small molecule–induced TIR-NB-LRR signaling induces root growth arrest via EDS1- and PAD4-complexed R protein VICTR in Arabidopsis. Plant Cell **24:** 5177–5192.

Letunic, I., and Bork, P. (2016). Interactive tree of life (iTOL) v3: An online tool for the display and annotation of phylogenetic and other trees. Nucleic Acids Res. **44:** W242–W245.

Li, L., Stoeckert, C.J., and Roos, D.S. (2003). OrthoMCL: Identification of ortholog groups for eukaryotic genomes. Genome Res. **13:** 2178–2189.

Liu, M.-J., et al. (2014). The complex jujube genome provides insights into fruit tree biology. Nat. Commun. **5:** 5315.

Liu, H., Ding, Y., Zhou, Y., Jin, W., Xie, K., and Chen, L.-L. (2017). CRISPR-P 2.0: An improved CRISPR-Cas9 tool for genome editing in plants. Mol. Plant **10:** 530–532.

Logemann, E., Birkenbihl, R.P., Ülker, B., and Somssich, I.E. (2006). An improved method for preparing Agrobacterium cells that simplifies the Arabidopsis transformation protocol. Plant Methods **2:** 16.

Meyers, B.C., Morgante, M., and Michelmore, R.W. (2002). TIR-X and TIR–NBS proteins: Two new families related to disease resistance TIR–NBS–LRR proteins encoded in Arabidopsis and other plant genomes. Plant J. **32:** 77–92.

Mine, A., Seyfferth, C., Kracher, B., Berens, M.L., Becker, D., and Tsuda, K. (2018). The defense phytohormone signaling network enables rapid, high-amplitude transcriptional reprogramming during effector-triggered immunity. Plant Cell **30:** 1199–1219.

Mitsuda, N., Ikeda, M., Takada, S., Takiguchi, Y., Kondou, Y., Yoshizumi, T., Fujita, M., Shinozaki, K., Matsui, M., and Ohme-Takagi, M. (2010). Efficient yeast one-/two-hybrid screening using a library composed only of transcription factors in Arabidopsis thaliana. Plant Cell Physiol. **51:** 2145–2151.

Ordon, J., Gantner, J., Kemna, J., Schwalgun, L., Reschke, M., Streubel, J., Boch, J., and Stuttmann, J. (2017). Generation of chromosomal deletions in dicotyledonous plants employing a user–friendly genome editing toolkit. Plant J. **89:** 155–168.

Peart, J.R., Mestre, P., Lu, R., Malcuit, I., and Baulcombe, D.C. (2005). NRG1, a CC-NB-LRR protein, together with N, a TIR-NB-LRR protein, mediates resistance against Tobacco mosaic virus. Curr. Biol. **15:** 968–973.

Peterson, B.A., Haak, D.C., Nishimura, M.T., Teixeira, P.J.P.L., James, S.R., Dangl, J.L., and Nimchuk, Z.L. (2016). Genome-wide assessment of efficiency and specificity in CRISPR/Cas9 mediated multiple site targeting in Arabidopsis. PLoS One **11:** e0162169.

Petrie, E.J., Czabotar, P.E., and Murphy, J.M. (2018). The structural basis of necroptotic cell death signaling. Trends Biochem. Sci. **44:** 53–63.

Pupko, T., Bell, R.E., Mayrose, I., Glaser, F., and Ben-Tal, N. (2002). Rate4Site: An algorithmic tool for the identification of functional regions in proteins by surface mapping of evolutionary determinants within their homologues. Bioinformatics **18:** S71–S77.

Qi, T., Seong, K., Thomazella, D.P.T., Kim, J.R., Pham, J., Seo, E., Cho, M.-J., Schultink, A., and Staskawicz, B.J. (2018). NRG1 functions downstream of EDS1 to regulate TIR-NLR-mediated plant immunity in *Nicotiana benthamiana.* Proc. Natl. Acad. Sci. USA **115:** E10979–E10987.

Rietz, S., Stamm, A., Malonek, S., Wagner, S., Becker, D., Medina-Escobar, N., Vlot, A.C., Feys, B.J., Niefind, K., and Parker, J.E. (2011). Different roles of Enhanced Disease Susceptibility1 (EDS1) bound to and dissociated from Phytoalexin Deficient4 (PAD4) in Arabidopsis immunity. New Phytol. **191:** 107–119.

Ronquist, F., and Huelsenbeck, J.P. (2003). MrBayes 3: Bayesian phylogenetic inference under mixed models. Bioinformatics **19:** 1572–1574.

Saucet, S.B., Ma, Y., Sarris, P.F., Furzer, O.J., Sohn, K.H., and Jones, J.D.G. (2015). Two linked pairs of Arabidopsis TNL resistance genes independently confer recognition of bacterial effector AvrRps4. Nat. Commun. **6:** 6338.

Schultink, A., Qi, T., Lee, A., Steinbrenner, A.D., and Staskawicz, B. (2017). Roq1 mediates recognition of the *Xanthomonas* and *Pseudomonas* effector proteins XopQ and HopQ1. Plant J. **92:** 787–795.

Schultink, A., Qi, T., Bally, J., and Staskawicz, B. (2019). Using forward genetics in *Nicotiana benthamiana* to uncover the immune signaling pathway mediating recognition of the *Xanthomonas perforans* effector XopJ4. New Phytol. **221:** 1001–1009.

Shao, Z.-Q., Xue, J.-Y., Wu, P., Zhang, Y.-M., Wu, Y., Hang, Y.-Y., Wang, B., and Chen, J.-Q. (2016). Large-scale analyses of angiosperm nucleotide-binding site-leucine-rich repeat genes reveal three anciently diverged classes with distinct evolutionary patterns. Plant Physiol. **170:** 2095–2109.

Sohn, K.H., Segonzac, C., Rallapalli, G., Sarris, P.F., Woo, J.Y., Williams, S.J., Newman, T.E., Paek, K.H., Kobe, B., and Jones, J.D.G. (2014). The nuclear immune receptor *RPS4* is required for *RRS1SLH1*-dependent constitutive defense activation in *Arabidopsis thaliana*. PLoS Genet. **10:** e1004655.

Stamatakis, A. (2014). RAxML version 8: A tool for phylogenetic analysis and post-analysis of large phylogenies. Bioinformatics **30:** 1312–1313.

Stuttmann, J., Hubberten, H.-M., Rietz, S., Kaur, J., Muskett, P., Guerois, R., Bednarek, P., Hoefgen, R., and Parker, J.E. (2011). Perturbation of Arabidopsis amino acid metabolism causes incompatibility with the adapted biotrophic pathogen *Hyaloperonospora arabidopsidis*. Plant Cell **23:** 2788–2803.

Talavera, G., and Castresana, J. (2007). Improvement of phylogenies after removing divergent and ambiguously aligned blocks from protein sequence alignments. Syst. Biol. **56:** 564–577.

Thieme, F., et al. (2005) Insights into genome plasticity and pathogenicity of the plant pathogenic bacterium *Xanthomonas campestris* pv. *vesicatoria* revealed by the complete genome sequence. J. Bacteriol. **187:** 7254–7266.

Tsuda, K., Mine, A., Bethke, G., Igarashi, D., Botanga, C.J., Tsuda, Y., Glazebrook, J., Sato, M., and Katagiri, F. (2013). Dual regulation of gene expression mediated by extended MAPK activation and salicylic acid contributes to robust innate immunity in Arabidopsis thaliana. PLoS Genet. **9:** e1004015.

Tsutsui, H., and Higashiyama, T. (2017). pKAMA-ITACHI vectors for highly efficient CRISPR/Cas9-mediated gene knockout in *Arabidopsis thaliana*. Plant Cell Physiol. **58:** 46–56.

VanBuren, R., Bryant, D., Bushakra, J.M., Vining, K.J., Edger, P.P., Rowley, E.R., Priest, H.D., Michael, T.P., Lyons, E., Filichkin, S.A., Dossett, M., and Finn, C.E., et al. (2016) The genome of black raspberry (Rubus occidentalis). Plant J. **87:** 535–547.

Van Der Biezen, E.A., Freddie, C.T., Kahn, K., Parker, J.E., and Jones, J.D.G. (2002). Arabidopsis *RPP4* is a member of the *RPP5* multigene family of *TIR-NB-LRR* genes and confers downy mildew resistance through multiple signalling components. Plant J. **29:** 439–451.

Venkat, A., Hahn, M.W., and Thornton, J.W. (2018). Multinucleotide mutations cause false inferences of lineage-specific positive selection. Nat. Ecol. Evol. **2:** 1280–1288.

Venugopal, S.C., Jeong, R.-D., Mandal, M.K., Zhu, S., Chandra-Shekara, A.C., Xia, Y., Hersh, M., Stromberg, A.J., Navarre, D., Kachroo, A., and Kachroo, P. (2009). Enhanced disease susceptibility 1 and salicylic acid act redundantly to regulate resistance gene-mediated signaling. PLoS Genet. **5:** e1000545.

Wagner, S., Stuttmann, J., Rietz, S., Guerois, R., Brunstein, E., Bautor, J., Niefind, K., and Parker, J.E. (2013). Structural basis for signaling by exclusive EDS1 heteromeric complexes with SAG101 or PAD4 in plant innate immunity. Cell Host Microbe **14:** 619–630.

Wiermer, M., Feys, B.J., and Parker, J.E. (2005). Plant immunity: The EDS1 regulatory node. Curr. Opin. Plant Biol. **8:** 383–389.

Wirthmueller, L., Zhang, Y., Jones, J.D.G., and Parker, J.E. (2007). Nuclear accumulation of the Arabidopsis immune receptor RPS4 is necessary for triggering EDS1-dependent defense. Curr. Biol. **17:** 2023–2029.

Witte, C.-P., Noël, L., Gielbert, J., Parker, J., and Romeis, T. (2004). Rapid one-step protein purification from plant material using the eight-amino acid StrepII epitope. Plant Mol. Biol. **55:** 135–147.

Wróblewski, T., Spiridon, L., Martin, E.C., Petrescu, A.-J., Cavanaugh, K., Truco, M.J., Xu, H., Gozdowski, D., Pawłowski, K., Michelmore, R.W., and Takken, F.L.W. (2018). Genome-wide functional analyses of plant coiled-coil NLR-type pathogen receptors reveal essential roles of their N-terminal domain in oligomerization, networking, and immunity. PLoS Biol. **16:** e2005821.

Wu, C.-H., Abd-El-Haliem, A., Bozkurt, T.O., Belhaj, K., Terauchi, R., Vossen, J.H., and Kamoun, S. (2017). NLR network mediates immunity to diverse plant pathogens. Proc. Nat. Acad. Sci. **114:** 8113–8118.

Wu, C.-H., Derevnina, L., and Kamoun, S. (2018). Receptor networks underpin plant immunity. Science **360:** 1300–1301.

Wu, Z., Li, M., Dong, O.X., Xia, S., Liang, W., Bao, Y., Wasteneys, G., and Li, X. (2019). Differential regulation of TNL-mediated immune signaling by redundant helper CNLs. New Phytol. **222:** 938–953.

Xu, F., Zhu, C., Cevik, V., Johnson, K., Liu, Y., Sohn, K., Jones, J.D., Holub, E.B., and Li, X. (2015). Autoimmunity conferred by chs3-2D relies on CSA1, its adjacent TNL-encoding neighbour. Sci. Rep. **5:** 8792.

Yang, Z. (2007). PAML 4: Phylogenetic analysis by maximum likelihood. Mol. Biol. Evol. **24:** 1586–1591.

Zhang, X., Dodds, P.N., and Bernoux, M. (2017). What do we know about NOD-like receptors in plant immunity? Annu. Rev. Phytopathol. **55:** 205–229.

Zhang, Y., Goritschnig, S., Dong, X., and Li, X. (2003). A gain-of-function mutation in a plant disease resistance gene leads to constitutive activation of downstream signal transduction pathways in *suppressor of npr1–1, constitutive 1*. Plant Cell **15:** 2636–2646.

Zhang, Y., Xia, R., Kuang, H., and Meyers, B.C. (2016). The diversification of plant NBS-LRR defense genes directs the evolution of microRNAs that target them. Mol. Biol. Evol. **33:** 2692–2705.

Zheng, X.-Y., Spivey, N.W., Zeng, W., Liu, P.-P., Fu, Z.Q., Klessig, D.F., He, S.Y., and Dong, X. (2012). Coronatine promotes *Pseudomonas syringae* virulence in plants by activating a signaling cascade that inhibits salicylic acid accumulation. Cell Host Microbe **11:** 587–596.

Zhong, Y., and Cheng, Z.-M. (2016). A unique RPW8-encoding class of genes that originated in early land plants and evolved through domain fission, fusion, and duplication. Sci. Rep. **6:** 32923.

Zhou, N., Tootle, T.L., Tsui, F., Klessig, D.F., and Glazebrook, J. (1998). PAD4 functions upstream from salicylic acid to control defense responses in Arabidopsis. Plant Cell **10:** 1021–1030.

Zou, C., et al. (2017). A high-quality genome assembly of quinoa provides insights into the molecular basis of salt bladder-based salinity tolerance and the exceptional nutritional value. Cell Res. **27:** 1327–1340.

A Coevolved EDS1-SAG101-NRG1 Module Mediates Cell Death Signaling by TIR-Domain Immune Receptors

Dmitry Lapin, Viera Kovacova, Xinhua Sun, Joram A. Dongus, Deepak Bhandari, Patrick von Born, Jaqueline Bautor, Nina Guarneri, Jakub Rzemieniewski, Johannes Stuttmann, Andreas Beyer and Jane E. Parker

This information is current as of November 28, 2019

Supplemental Data	/content/suppl/2019/07/16/tpc.19.00118.DC1.html /content/suppl/2019/11/09/tpc.19.00118.DC2.html
References	This article cites 90 articles, 20 of which can be accessed free at: /content/31/10/2430.full.html#ref-list-1
Permissions	https://www.copyright.com/ccc/openurl.do?sid=pd_hw1532298X&issn=1532298X&WT.mc_id=pd_hw1532298X
eTOCs	Sign up for eTOCs at: http://www.plantcell.org/cgi/alerts/ctmain
CiteTrack Alerts	Sign up for CiteTrack Alerts at: http://www.plantcell.org/cgi/alerts/ctmain
Subscription Information	Subscription Information for *The Plant Cell* and *Plant Physiology* is available at: http://www.aspb.org/publications/subscriptions.cfm